

Nonhermitean Random Matrix Models

Romuald A. Janik^a, Maciej A. Nowak^{a,b,c}, Gábor Papp^{b,d} and
Ismail Zahed^e

^a*Department of Physics, Jagellonian University, 30-059 Kraków, Poland*

^b*GSI, Plankstr. 1, D-64291 Darmstadt, Germany*

^c*Institut für Kernphysik, TH Darmstadt, D-64289 Darmstadt, Germany*

^d*Institute for Theoretical Physics, Eötvös University, Budapest, Hungary*

^e*Department of Physics, SUNY, Stony Brook, New York 11794, USA.*

Abstract

We introduce an extension of the diagrammatic rules in random matrix theory and apply it to nonhermitean random matrix models using the $1/N$ approximation. A number of one- and two-point functions are evaluated on their holomorphic and non-holomorphic supports to leading order in $1/N$. The one-point functions describe the distribution of eigenvalues, while the two-point functions characterize their macroscopic correlations. Generic form for the two-point functions are obtained, generalizing the concept of macroscopic universality to nonhermitean random matrices. We show that the holomorphic and nonholomorphic one- and two-point functions condition the behavior of pertinent partition functions to order $\mathcal{O}(1/N)$. We derive explicit conditions for the location and distribution of their singularities. Most of our analytical results are found to be in good agreement with numerical calculations using large ensembles of complex matrices.

PACS: 05.40.+j; 05.45+b; 05.70.Fh; 11.15.Pg

Keywords: Nonhermitean random matrix models, Diagrammatic expansion, Universal correlator

Contents

1	Introduction	3
2	Hermitean Random Ensembles	4
2.1	Pastur Equation	5
2.2	Chiral Pastur Equations	6
2.3	Random Dirac Operators	8
3	Nonhermitean Random Ensembles	8
3.1	Example	10
3.2	Diagrammatic rules	10
4	One-Point Functions	11
4.1	Pure Complex Random Matrices	11
4.2	Real Asymmetric (Square) Matrices	13
4.3	Nonhermitean Chiral Matrices	14
4.4	Random Scattering Model	16
5	Two-Point Functions	20
5.1	Notations	21
5.2	Ginibre-Girko Correlator	22
5.3	Elliptic Correlator	25
5.4	Chiral Correlator I (Holomorphic Region)	28
5.5	Chiral Correlator II (Non-Holomorphic Region)	30
5.6	Scattering Correlator	33
6	Partition Functions	36
6.1	Holomorphic Z	37
6.2	Nonholomorphic Z	42
7	Conclusions	45
	Acknowledgements	46
	References	46

1 Introduction

Random matrix models provide an interesting setup for modeling a number of physical phenomena, where noise plays a prominent role. Applications range from atomic physics to quantum gravity. In these phenomena, one may distinguish between the universal behavior of noise exhibited as fluctuations at the mesoscopic scale (microscopic universality) and the macroscopic scale (macroscopic universality) in bulk systems with or without absorption. Simple physical realizations of these universalities are encountered in disordered mesoscopic systems [1].

In this work, we will be concerned with the generic behavior of two classes of random matrix models: those without dissipation (hermitean) and those with dissipation (nonhermitean). Since conventional hermitean matrix ensembles have been considerably investigated [2] (For recent discussion on macroscopic correlators see e.g. [3]), we will keep our discussion to the chiral unitary ensembles [4], and we devote most of our studies to nonhermitean ensembles, which are less known although they play an increasingly important role in quantum problems [5,6].

A number of methods have been devised to calculate with random matrix models. Most prominent perhaps are the Schwinger-Dyson approach [7] and the supersymmetric method [8]. In this paper, we would like to elaborate on diagrammatic techniques for a variety of random matrix models, with special focus on the chiral and nonhermitean ensembles. The use of diagrammatic methods in random matrix models is not new, although those methods were not previously applied to nonhermitean matrices, and we refer the reader to [9] (and references therein). In this work we will discuss one- and two-point functions. They carry information on the eigenvalue distributions and their (macroscopic) correlations. They involve singular operators in the large N limit, and in general break spontaneously holomorphic symmetry. We show also that they condition in a simple way the character of pertinent partition functions to order $\mathcal{O}(1/N)$, as in general expected.

The organization of this paper is as follows: in section 2, we set up the notations for the hermitean case, and evaluate the resolvent in the $1/N$ approximation. We show how the result changes in the chiral case, and apply it to a schematic version of a Dirac operator. In section 3, we extend our diagrammatic arguments to the nonhermitean case, using real and nonhermitean random matrix models as an example. The important difference between hermitean and nonhermitean matrix models, is the possibility of spontaneous breaking of holomorphic symmetry in the eigenvalue plane. In section 4, we work out the resolvents in the case of real and asymmetric matrices, nonhermitean chiral matrices and a random scattering model. In section 5, we evaluate a number of

two-point correlators. We show that they all follow the general lore of macroscopic universality, thereby generalizing the idea of Ambjørn, Jurkiewicz and Makeenko [10] and also Brézin and Zee [11] to the nonhermitean case. All our results are found in good agreement with large scale numerical calculations. In section 6, we show that the one- and two-point functions may be used to generate pertinent partition functions to order $\mathcal{O}(1/N)$ for both the holomorphic as well as nonholomorphic case. We use the Ginibre-Girko ensembles [12], as a way of illustration. A Straightforward generalization to other unitary ensembles is briefly mentioned. Our conclusions are summarized in section 7.

2 Hermitean Random Ensembles

To illustrate the arguments and set up the notation for the diagrammatic arguments to follow, let us first consider the well known case of a deterministic plus random hermitean ensemble with Gaussian distribution. It is convenient to use the diagrammatic notation introduced by [11], borrowing on the standard large N diagrammatics for QCD [14]. For the random part, the fermionic Lagrangian is simply

$$\mathcal{L} = \bar{\psi}_a (z \mathbf{1}_a^b - H_a^b) \psi^b, \quad (2.1)$$

where H is a hermitean random matrix with Gaussian weight. We will refer to ψ as a “quark” and to H as a “gluon”. The “Feynman graphs” following from (2.1) allow only for the flow of “color” (no momentum), since (2.1) defines a field-theory in $0 + 0$ dimensions. They are an efficient way of keeping track of “color” factors.¹ The “quark” and “gluon” propagators (double line notation) are shown in Fig. 2.1. For hermitean random matrices the Gaussian averaging preserves holomorphic symmetry in the large N limit. This is not the case for nonhermitean random matrices when singular operators are considered (see sections 3-6).

Fig. 2.1. Large N “Feynman” rules for “quark” and “gluon” propagators.

¹ The names “quarks”, “gluons”, “color” etc. are used here in a figurative sense, without any connection to QCD. In order to avoid any confusion, we always use these names in quotation marks.

2.1 Pastur Equation

The pertinent resolvent for (2.1) is given by [11,15,16]

$$G(z) := \frac{1}{N} \langle \text{tr} \frac{1}{z - D - \mathcal{H}} \rangle, \quad (2.2)$$

where \mathcal{H} is an $N \times N$ hermitean random matrix, and D a deterministic part. The distribution of eigenvalues $\nu(z)$ of $H = D + \mathcal{H}$ follows from (2.2) through $\pi\nu(z) = \partial_{\bar{z}}G$.

Throughout, the weight average is considered Gaussian for simplicity. However, all our arguments generalize to the non-Gaussian weight. In terms of the one-particle irreducible self energy $\tilde{\Sigma}$, (2.2) reads

$$G(z) = \frac{1}{N} \text{tr} \frac{1}{z - D - \tilde{\Sigma}}. \quad (2.3)$$

We note that since the argument in (2.2) displays poles on the real axis only (hermitean matrices), it is safe to assume that after averaging and in large N , the resolvent is holomorphic in the z -plane modulo possible singularities on the real axis, for which $\nu(z) \neq 0$. This property is manifest in (2.3).

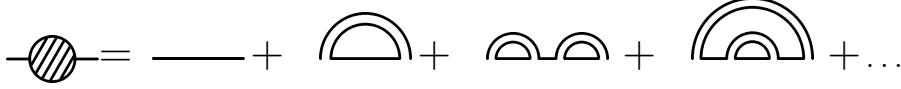


Fig. 2.2. Rainbow diagrams.

In the large N limit the equation for the self energy $\tilde{\Sigma}$ follows from resumming the rainbow diagrams of Fig. 2.2. All other diagrams (non-planar) are subleading in the large N limit. The result is

$$\left(\frac{1}{z - D - \tilde{\Sigma}} \right)_{bc} \mathcal{D}_{ab,cd} = \tilde{\Sigma}_{ad} \quad (2.4)$$

where $\mathcal{D}_{ab,cd}$ is the random matrix propagator given by

$$\mathcal{D}_{ab,cd} = \langle \mathcal{H}_b^a \mathcal{H}_d^c \rangle = \frac{1}{N} \delta_{ad} \delta_{bc}. \quad (2.5)$$

Inserting this into (2.4) we find that $\tilde{\Sigma} = \Sigma \cdot \mathbf{1}$, where $\mathbf{1}$ is the identity matrix, and Σ is a scalar satisfying Pastur's equation (see Fig. 2.3)

$$\frac{1}{N} \text{tr} \frac{1}{z - D - \Sigma} = \Sigma. \quad (2.6)$$

We note that $\Sigma = G(z)$. It is convenient, for the generalization to the chiral case, to represent the propagator as a tensor product of matrices

$$\mathcal{D} = \mathbf{1} \otimes \mathbf{1}. \quad (2.7)$$

As a result equation (2.4) becomes

$$\frac{1}{N} \text{tr} \left[\frac{1}{z - D - \tilde{\Sigma}} \mathbf{1} \right] \otimes \mathbf{1} = \tilde{\Sigma}. \quad (2.8)$$

This result was derived by a number of authors [11,15,16].

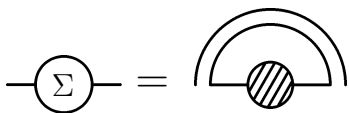


Fig. 2.3. Pastur equation.

2.2 Chiral Pastur Equations

In the chiral case the $0 + 0$ dimensional Lagrangian (2.1) becomes

$$\mathcal{L} = \bar{\psi}_a (z \delta_a^b - \mathcal{M}_a^b) \psi^b \quad (2.9)$$

with the chiral random matrix

$$\mathcal{M} = \begin{pmatrix} 0 & \mathcal{R} \\ \mathcal{R}^\dagger & 0 \end{pmatrix}. \quad (2.10)$$

Here, the “quarks” are chiral in the sense that $\psi = (\psi_R, \psi_L)$, following the block decomposition in (2.10). The chirality operator is

$$\gamma_5 = \begin{pmatrix} \mathbf{1} & 0 \\ 0 & -\mathbf{1} \end{pmatrix}. \quad (2.11)$$

We may now apply the results of the previous section but with a different propagator. Namely

$$\mathcal{D}_{ab,cd} = \langle \mathcal{M}_b^a \mathcal{M}_d^c \rangle = \frac{1}{N} \delta_{ad} \delta_{bc} \quad a > N, b < N \text{ or } a < N, b > N \quad (2.12)$$

and zero otherwise. In the tensor product notation we get

$$\mathcal{D} = \frac{1}{N} \begin{pmatrix} \mathbf{1} & 0 \\ 0 & 0 \end{pmatrix} \otimes \begin{pmatrix} 0 & 0 \\ 0 & \mathbf{1} \end{pmatrix} + \frac{1}{N} \begin{pmatrix} 0 & 0 \\ 0 & \mathbf{1} \end{pmatrix} \otimes \begin{pmatrix} \mathbf{1} & 0 \\ 0 & 0 \end{pmatrix}. \quad (2.13)$$

Again, the random averaging is carried using a Gaussian weight. Since (2.9) is chirally symmetric for $z = 0$, the question arises as to whether the averaging breaks spontaneously chiral symmetry in the large N limit. This is indeed the case for $z \rightarrow i0$ after $N \rightarrow \infty$. Inserting (2.13) into equation (2.4) we obtain

$$\begin{aligned} & \frac{1}{N} \text{tr} \left[\frac{1}{z - D - \tilde{\Sigma}} \begin{pmatrix} \mathbf{1} & 0 \\ 0 & 0 \end{pmatrix} \right] \otimes \begin{pmatrix} 0 & 0 \\ 0 & \mathbf{1} \end{pmatrix} \\ & + \frac{1}{N} \text{tr} \left[\frac{1}{z - D - \tilde{\Sigma}} \begin{pmatrix} 0 & 0 \\ 0 & \mathbf{1} \end{pmatrix} \right] \otimes \begin{pmatrix} \mathbf{1} & 0 \\ 0 & 0 \end{pmatrix} = \tilde{\Sigma}. \end{aligned} \quad (2.14)$$

We see that $\tilde{\Sigma}$ is diagonal

$$\tilde{\Sigma} = \begin{pmatrix} \Sigma_1 \cdot \mathbf{1} & 0 \\ 0 & \Sigma_2 \cdot \mathbf{1} \end{pmatrix} \quad (2.15)$$

with Σ_1 and Σ_2 scalars and the Green's function is $G(z) = \frac{1}{2}(\Sigma_1 + \Sigma_2)$. The chiral Pastur's equations now take the form

$$\frac{1}{N} \text{tr} \left[\frac{1}{z - D - \tilde{\Sigma}} \begin{pmatrix} 0 & 0 \\ 0 & \mathbf{1} \end{pmatrix} \right] = \Sigma_1, \quad (2.16)$$

$$\frac{1}{N} \text{tr} \left[\frac{1}{z - D - \tilde{\Sigma}} \begin{pmatrix} \mathbf{1} & 0 \\ 0 & 0 \end{pmatrix} \right] = \Sigma_2. \quad (2.17)$$

As $z \rightarrow i0$, $\Sigma_1 = \Sigma_2 \neq 0$ implying that in the large N limit, the Gaussian averaging breaks spontaneously chiral symmetry. This is particularly interesting as it shows the following: the mechanism of spontaneous symmetry breakdown requires minimally that the interaction is chirally symmetric and random, a point presently embodied in the instanton vacuum description [17]. A related idea was first discussed in [18].

2.3 Random Dirac Operators

As an illustration of the above equations, consider the schematic case of chiral fermions with mass m . In this case, the deterministic $2N \times 2N$ matrix is

$$D = \begin{pmatrix} m & 0 \\ 0 & -m \end{pmatrix}. \quad (2.18)$$

Rearranging the rows and columns of the matrix $z - D - \tilde{\Sigma}$ and inverting, yield the following equations for Σ_1 and Σ_2

$$\begin{aligned} \Sigma_1 &= \frac{z - m - \Sigma_1}{(z - m - \Sigma_1)(z + m - \Sigma_2)}, \\ \Sigma_2 &= \frac{z + m - \Sigma_2}{(z - m - \Sigma_1)(z + m - \Sigma_2)}. \end{aligned} \quad (2.19)$$

Using the fact that $\Sigma_2/\Sigma_1 = (z + m)/(z - m)$ and $G = (\Sigma_1 + \Sigma_2)/2$ we get the equation for the Green's function

$$(G^3 - 2zG^2)(m^2 - z^2) + Gz^2(m^2 - (z^2 + 1)) + z^3 = 0. \quad (2.20)$$

We note that when $m = 0$ this gives exactly z^3 times the ordinary – hermitean – Pastur's equation for this case. Solving for Σ_1 gives

$$G = \frac{z}{2} \left(1 + \frac{\sqrt{z^2 - m^2 - 4}}{\sqrt{z^2 - m^2}} \right) \quad (2.21)$$

which is holomorphic in the z -plane modulo cuts on the real axis. The solutions to (2.19) were used in [19].

3 Nonhermitean Random Ensembles

If we were to use nonhermitean matrices in the resolvent (2.2), then configuration by configuration, the resolvent displays poles that are scattered around $z = 0$ (for $D = 0$) in the complex z -plane. Their spread is given by the Gaussian distribution, which is of order one. In the large N limit, the poles accumulate in general on finite surfaces (for unitary matrices on circles), over which the resolvent is no longer holomorphic. The (spontaneous) breaking of holomorphic symmetry follows from the large N limit. As a result $\partial G/\partial \bar{z} \neq 0$

on the nonholomorphic surface, with a finite eigenvalue distribution. In this section we will set up the diagrammatic rules for investigating nonhermitean random matrix models.

For hermitean matrices, “quarks” ψ and “conjugate-quarks” ϕ decouple in the “thermodynamical” limit ($N \rightarrow \infty$). Their respective resolvents follow from the $0 + 0$ dimensional Lagrangian

$$\mathcal{L}_0 = \bar{\psi}(z - \mathcal{M})\psi + \bar{\phi}(\bar{z} - \mathcal{M}^\dagger)\phi \quad (3.1)$$

and do not ‘talk’ to each other. They are holomorphic (antiholomorphic) functions modulo cuts on the real axis. For nonhermitean matrices, this is not the case in the large N limit. The spontaneous breaking of holomorphic symmetry in the large N limit, may be probed in the z -plane by adding to (3.1)

$$\mathcal{L}_B = \lambda(\bar{\psi}\phi + \bar{\phi}\psi) \quad (3.2)$$

in the limit $\lambda \rightarrow 0$. The combination $\mathcal{L}_0 + \mathcal{L}_B$ will be used below to investigate a number of random and nonhermitean ensembles with or without deterministic parts.

From (3.1,3.2) we define the matrix-valued resolvent through

$$\begin{pmatrix} \mathcal{G}_{qq} & \mathcal{G}_{q\bar{q}} \\ \mathcal{G}_{\bar{q}q} & \mathcal{G}_{\bar{q}\bar{q}} \end{pmatrix} = \left\langle \begin{pmatrix} z - \mathcal{M} & \lambda \\ \lambda & \bar{z} - \mathcal{M}^\dagger \end{pmatrix}^{-1} \right\rangle \quad (3.3)$$

where the limit $N \rightarrow \infty$ is understood before $\lambda \rightarrow 0$. For convenience, the “quark” field is organized in an isodoublet $\xi = (\psi, \phi) = (q, \bar{q})$. The “quark” spectral density follows from Gauss law,

$$\nu(z, \bar{z}) = \frac{1}{\pi} \partial_{\bar{z}} G(z, \bar{z}) = \frac{1}{\pi N} \partial_{\bar{z}} \text{Tr}_N \mathcal{G}_{qq} \quad (3.4)$$

which is the distribution of eigenvalues of \mathcal{M} . For hermitean \mathcal{M} , (3.4) is valued on the real axis. As $\lambda \rightarrow 0$, the block-structure decouples, and we are left with the original resolvent. For $z \rightarrow +i0$, the latter is just a measurement of the real eigenvalue distribution. For nonhermitean \mathcal{M} , (3.4) is valued in the z -plane. As $\lambda \rightarrow 0$, the block structure does not decouple, leading to a non-holomorphic resolvent for certain parts of the z -plane. Holomorphic symmetry is spontaneously broken in the large N limit. The size of the nonholomorphic regions is conditioned by the divergence of the “quark-conjugate-quark” two-point function (see below).

3.1 Example

To set up the diagrammatic rules we will use an example. Consider the case of real and nonhermitean matrices with off-diagonal correlations. Specifically, let M be a real and asymmetric $N \times N$ matrix so that

$$\langle M_{ij}^2 \rangle = \frac{1}{N} \quad \langle M_{ij} M_{ji} \rangle = \frac{\tau}{N}. \quad (3.5)$$

The case $\tau = 1$ reduces to symmetric real matrices. The random ensemble described by (3.5) occur naturally in neural network problems, and have been discussed in [20] using the replica construction.

3.2 Diagrammatic rules

From (3.1,3.2) we note that there are two kinds of “quark” propagators ($1/z$ for “quarks” ψ and $1/\bar{z}$ for “conjugate-quarks” ϕ , where both can be incoming and outgoing) and four kinds of “gluon” propagators, associated to the following “quark-conjugate-quark” amplitudes (treating the “quarks” as external sources)

$$\begin{aligned} \langle \bar{\psi}_b M_a^b \psi^a \bar{\psi}_c M_d^c \psi^d \rangle &= \bar{\psi}_b \psi^a \bar{\psi}_c \psi^d \langle M_a^b M_d^c \rangle \\ \langle \bar{\psi}_b M_a^b \psi^a \bar{\phi}_c (M^T)_d^c \phi^d \rangle &= \bar{\psi}_b \psi^a \bar{\phi}_c \phi^d \langle M_a^b (M^T)_d^c \rangle \\ \langle \bar{\phi}_b (M^T)_a^b \phi^a \bar{\psi}_c M_d^c \psi^d \rangle &= \bar{\phi}_b \phi^a \bar{\psi}_c \psi^d \langle (M^T)_a^b M_d^c \rangle \\ \langle \bar{\phi}_b (M^T)_a^b \phi^a \bar{\phi}_c (M^T)_d^c \phi^d \rangle &= \bar{\phi}_b \phi^a \bar{\phi}_c \phi^d \langle (M^T)_a^b (M^T)_d^c \rangle. \end{aligned} \quad (3.6)$$

In each of these four cases, averaging is done with the weight

$$\langle \dots \rangle = \int [dM] \exp \left[-\frac{N}{2(1-\tau^2)} \text{tr}(MM^T - \tau MM) \right] \quad (3.7)$$

reproducing the correlations (3.5). Indeed,

$$\langle M_b^a M_c^d \rangle = \frac{1}{N} (\delta_{bc} \delta^{ad} + \tau \delta_b^d \delta_c^a) \quad (3.8)$$

where the second contribution corresponds to twisting the lines with a “penalty factor” τ . For $\tau = \pm 1$ this is equivalent to symmetrizing or antisymmetrizing the double lines in the “gluon” propagator. All combinations arising from the averaging (3.7) are shown in Fig. 3.1. The pairs (ae),(bf), (cg) and (dh) in Fig. 3.1 correspond to four “gluon” propagators, evaluated with the weight

(3.7). The lower row in Fig. 3.1 corresponds to terms with $\tau \neq 0$. The arrows denote incoming and outgoing particles, the “quarks” and “conjugate-quarks” are distinguished by their labels.

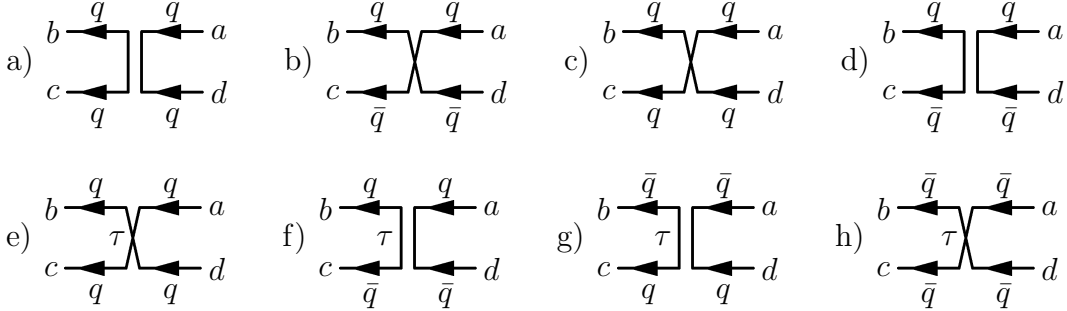


Fig. 3.1. All “gluonic” amplitudes for real nonhermitean matrices.

The generalization to the hermitean-antihermitean case, i.e. the case of complex matrices, corresponds to the substitution $M^T \rightarrow M^\dagger$ with the measure

$$\langle \dots \rangle = \int [dM] \exp \left[-\frac{N}{(1-\tau^2)} \text{tr}(MM^\dagger - \tau \text{Re}MM) \right]. \quad (3.9)$$

The relations (3.5) should be replaced by

$$\langle |M_{ab}|^2 \rangle = \frac{1}{N} \quad \langle M_{ab}M_{ba} \rangle = \frac{\tau}{N} \quad (3.10)$$

corresponding to hermitean ($\tau = 1$), antihermitean ($\tau = -1$) or general complex ($\tau = 0$) matrix theory. In the latter the relevant “gluonic” amplitudes correspond now to Fig. 3.1a–3.1d.

4 One-Point Functions

In this section we will explicitly calculate a number of one-point functions (resolvents) for several nonhermitean random matrix models, using and extending when needed the diagrammatic approach discussed above.

4.1 Pure Complex Random Matrices

We seek the one-point functions for $\langle \bar{\xi}_i \xi_j \rangle$ as a 2×2 matrix. The equation for the one particle irreducible (1PI) self-energy follows from Figs. 3.1–4.1 in the form

$$\begin{aligned}
\begin{pmatrix} \Sigma_1 & \Sigma_2 \\ \Sigma_3 & \Sigma_4 \end{pmatrix} &= \frac{1}{N} \text{tr}_N \begin{pmatrix} \mathcal{G}_{qq} & \mathcal{G}_{q\bar{q}} \\ \mathcal{G}_{\bar{q}q} & \mathcal{G}_{\bar{q}\bar{q}} \end{pmatrix} \circ \begin{pmatrix} \tau & 1 \\ 1 & \tau \end{pmatrix} \\
&= \frac{1}{N} \text{tr}_N \begin{pmatrix} z - \Sigma_1 & \lambda - \Sigma_2 \\ \lambda - \Sigma_3 & \bar{z} - \Sigma_4 \end{pmatrix}^{-1} \circ \begin{pmatrix} \tau & 1 \\ 1 & \tau \end{pmatrix}.
\end{aligned} \tag{4.1}$$

Here the trace is meant component-wise (block per block), and the argument of the trace is the dressed propagator. The operation \circ is *not* a matrix multiplication, but a simple multiplication between the entries in the corresponding positions. Here tr_N is short for the trace on the $N \times N$ block-matrices.

The first correlator in (3.5) does not influence the ‘‘quark-quark’’ interaction - it corresponds to the double line with a twist in the corresponding Pastur equation - hence subleading. However, this twist could be compensated by the twisted part of the propagator coming from the second correlator (3.5), thereby explaining the factor τ in the upper left corner of (4.1). This is shown in Fig. 4.1, where the first (subleading) graph comes from Fig. 3.1a and the second (leading) comes from Fig. 3.1e. The other entries in (4.1) follow from Fig. 3.1 by inspection.

The ‘‘quark’’ one-point function is now

$$G(z, \bar{z}) = \frac{1}{N} \text{tr}_N \mathcal{G}_{qq} = (\bar{z} - \Sigma_4) / \det. \tag{4.2}$$

It follows that $\Sigma_2 = \Sigma_3$, with

$$\det \Sigma_1 = \tau(\bar{z} - \Sigma_4) \tag{4.3}$$

$$\det \Sigma_4 = \tau(z - \Sigma_1) \tag{4.4}$$

$$\det \Sigma_2 = \Sigma_2 - \lambda, \tag{4.5}$$

where $\det = (z - \Sigma_1)(\bar{z} - \Sigma_4) - (\lambda - \Sigma_2)^2$. Substituting $r = \Sigma_2 - \lambda$ in the last relation in (4.5) yields the equation

$$((z - \Sigma_1)(\bar{z} - \Sigma_4) - r^2)(r + \lambda) = r. \tag{4.6}$$

For $\lambda = 0$, the solution with $r = 0$ is holomorphic while that with $r \neq 0$ is nonholomorphic. In the holomorphic case, $\Sigma_1(z - \Sigma_1) = \tau$, and the resolvent is simply

$$G(z) = \frac{z \mp \sqrt{z^2 - 4\tau}}{2\tau}. \tag{4.7}$$

where the upper sign corresponds to the solution with the pertinent asymptotics. In the nonholomorphic case, $G(z, \bar{z}) = \bar{z} - \Sigma_4$, with

$$G(z, \bar{z}) = \frac{\bar{z} - \tau z}{1 - \tau^2} \quad (4.8)$$

in agreement with [20]. The boundary between the holomorphic and nonholomorphic solution follows from the condition $|G(z, \bar{z})|^2 = |G(z)|^2 = 1$, that is

$$\frac{x^2}{(1 + \tau)^2} + \frac{y^2}{(1 - \tau)^2} = 1 \quad (4.9)$$

which is an ellipse. Inside (4.9) the solution is nonholomorphic and outside it is holomorphic. The case investigated by Ginibre and Girko [12] follows for $\tau = 0$. The one-point function for the random matrix $(H_1 + iH_2)/\sqrt{2}$ can be obtained similarly. The self-energy equation being the same as before but with $\tau = 0$.

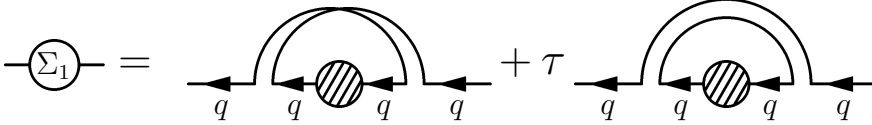


Fig. 4.1. Self-energy equation for real nonhermitean matrices.

4.2 Real Asymmetric (Square) Matrices

Following Khoruzhenko [21] we define the random matrix ensemble

$$H_0 + A \quad (4.10)$$

where H_0 is a deterministic but otherwise arbitrary (e.g. complex) matrix and A is a real asymmetric random matrix with

$$\langle a_{jk} a_{lm} \rangle = \frac{1}{N} v^2 \delta_{jl} \delta_{km}. \quad (4.11)$$

The 1PI self energy equations are now

$$\begin{pmatrix} \Sigma_1 & \Sigma_2 \\ \Sigma_3 & \Sigma_4 \end{pmatrix} = \text{tr}_N \left(\begin{pmatrix} z - H_0 - \Sigma_1 & \lambda - \Sigma_2 \\ \lambda - \Sigma_3 & \bar{z} - H_0^\dagger - \Sigma_4 \end{pmatrix}^{-1} \circ \begin{pmatrix} 0 & v^2 \\ v^2 & 0 \end{pmatrix} \right). \quad (4.12)$$

Care must be taken with the definition of the inverse matrix. The inverse is taken only with respect to the “isospin” indices (2×2), so the determinant is now a matrix in N-space. We obtain

$$\begin{pmatrix} \Sigma_1 & \Sigma_2 \\ \Sigma_3 & \Sigma_4 \end{pmatrix} = \text{tr}_N \begin{pmatrix} \bar{z} - H_0^\dagger - \Sigma_4 & \Sigma_2 - \lambda \\ \Sigma_3 - \lambda & z - H_0 - \Sigma_1 \end{pmatrix} \circ \begin{pmatrix} 0 & v^2 D_R^{-1} \\ v^2 D_L^{-1} & 0 \end{pmatrix} \quad (4.13)$$

with $\Sigma_2 = \Sigma_3 = x$ for $\lambda = 0$ and

$$\begin{aligned} D_L &= (\bar{z} - H_0^\dagger - \Sigma_4)(z - H_0 - \Sigma_1) - x^2, \\ D_R &= (z - H_0 - \Sigma_1)(\bar{z} - H_0^\dagger - \Sigma_4) - x^2 \end{aligned} \quad (4.14)$$

since we do not impose that H_0 and H_0^\dagger commute. We see that $\Sigma_1 = \Sigma_4 = 0$ and the equation for $\Sigma_2 = x$ now has the form

$$x = v^2 \cdot x \cdot \frac{1}{N} \text{tr}_N [(\bar{z} - H_0^\dagger)(z - H_0) - x^2]^{-1}. \quad (4.15)$$

The solution with $x \neq 0$ corresponds to the non-analytical Green’s function. Its “quark” Green’s function is given by

$$G(z, \bar{z}) = \frac{1}{N} \text{tr}_N [(\bar{z} - H_0^\dagger)G_0(-x^2)] \quad (4.16)$$

where $G_0(w)$ is the generalized resolvent

$$G_0(w) = \frac{1}{(\bar{z} - H_0^\dagger)(z - H_0) + w} \quad (4.17)$$

and x satisfies

$$\frac{1}{N} \text{tr}_N G_0(-x^2) = \frac{1}{v^2}. \quad (4.18)$$

These are the equations obtained by Khoruzhenko [21].

4.3 Nonhermitean Chiral Matrices

In this section we will reanalyze the chiral random matrix model of section 2.2 in the presence of a nonhermitean part, *e.g.* “chemical potential” μ . The motivation for that stems from the constant mode sector of the massless and chiral

Dirac operator at finite chemical potential [22]. Here we will use Gaussian chiral and random matrices as described by (3.1).

If we were to define

$$\gamma = i\gamma_0 = \begin{pmatrix} 0 & -1 \\ 1 & 0 \end{pmatrix} \quad \text{and} \quad \mathcal{M} = \begin{pmatrix} 0 & -\mu + \mathcal{R} \\ \mu + \mathcal{R}^\dagger & 0 \end{pmatrix} \quad (4.19)$$

then the 1PI self-energy equations in the planar approximation are given by

$$\begin{pmatrix} \Sigma_1 & \Sigma_2 \\ \Sigma_3 & \Sigma_4 \end{pmatrix} = \frac{1}{N} \text{tr}_N \underbrace{\begin{pmatrix} z - \mu\gamma - \Sigma_1 & \lambda - \Sigma_2 \\ \lambda - \Sigma_3 & \bar{z} + \mu\gamma - \Sigma_4 \end{pmatrix}^{-1}}_{\mathcal{G}} \circ \begin{pmatrix} \mathcal{D} & \mathcal{D} \\ \mathcal{D} & \mathcal{D} \end{pmatrix} \quad (4.20)$$

where \mathcal{D} is the “gluon” propagator (2.12), and Σ_i are diagonal $2N \times 2N$ matrices. Inverting in (4.20) with respect to the “isospin” indices gives

$$\begin{pmatrix} \Sigma_1 & \Sigma_2 \\ \Sigma_3 & \Sigma_4 \end{pmatrix} = \text{tr}_N \begin{pmatrix} \bar{z} + \mu\gamma - \Sigma_4 & \Sigma_2 - \lambda \\ \Sigma_3 - \lambda & z - \mu\gamma - \Sigma_1 \end{pmatrix} \cdot \Delta^{-1} \circ \begin{pmatrix} \mathcal{D} & \mathcal{D} \\ \mathcal{D} & \mathcal{D} \end{pmatrix}. \quad (4.21)$$

Here Δ is the determinant of the 2×2 matrix with $2N \times 2N$ entries. The equation for $\Sigma_2 \neq 0$ in (4.21) gives

$$1 = \frac{1}{N} \text{tr} \left(\Delta^{-1} \cdot \mathcal{D} \right) \quad (4.22)$$

with

$$\Delta^{-1} = \begin{pmatrix} 1 & -\mu(\bar{z} - \Sigma_4 - z + \Sigma_1)/\alpha \\ \mu(\bar{z} - \Sigma_4 - z + \Sigma_1)/\alpha & 1 \end{pmatrix} \quad (4.23)$$

and where α^{2N} is the determinant of the $2N \times 2N$ matrix Δ . Inserting (4.23) into (4.21) yields

$$\Sigma_4 = z - \Sigma_1 - \mu^2 \frac{\bar{z} - \Sigma_4 - z + \Sigma_1}{\alpha} \quad (4.24)$$

$$\Sigma_1 = \bar{z} - \Sigma_4 + \mu^2 \frac{\bar{z} - \Sigma_4 - z + \Sigma_1}{\alpha}. \quad (4.25)$$

In particular $\Sigma_1 + \Sigma_4 = \text{Re } z \equiv x$. The resolvent for the “quark-quark” part is simply Σ_1 . Solving (4.25) in conjunction with (4.22) gives

$$\alpha^2 - \alpha + \mu^2(\bar{z} - \Sigma_4 - z + \Sigma_1)^2 = 0. \quad (4.26)$$

Simple algebra for the “quark-quark” resolvent gives

$$G(z, \bar{z}) = \frac{1}{2N} \text{tr}_N \mathcal{G}_{qq} = \frac{x}{2} - iy - \frac{1}{2} \frac{iy}{y^2 - \mu^2} \quad (4.27)$$

a result first derived in [23] using different arguments.

For $\Sigma_2 = 0$ we recover the holomorphic solution [23,34], $\Sigma_1(z) = G(z)\mathbf{1}$, $\Sigma_4 = \Sigma_1^\dagger$, with $G(z)$ fulfilling the cubic Pastur equation

$$G^3(z) - 2zG^2(z) + (z^2 + \mu^2 + 1)G(z) - z = 0. \quad (4.28)$$

4.4 Random Scattering Model

As a final application of the techniques introduced above, we consider the random matrix model discussed by Mahaux and Weidenmüller [24] in the context of chaotic resonance scattering. The model is generically described by a nonhermitean Hamiltonian of the form

$$H - i\gamma VV^\dagger \quad (4.29)$$

where H is random Gaussian (orthogonal) and $N \times N$ matrix-valued, while V is $N \times M$ matrix-valued [6,25]. The form (4.29) is dictated by unitarity. The V propagator is given by

$$\langle V_k^a V_l^b \rangle = \frac{1}{N} \delta^{ab} \delta_{kl}. \quad (4.30)$$

Fig. 4.2. Vertex corresponding to the VV^\dagger terms in the Hamiltonian.

In the following we will use the notation $\delta = i\gamma$ and $m = M/N$. The quadratic appearance of V in (4.30) calls for additional changes in the preceding Feynman rules. In particular, the 1PI self-energy has two new contributions:

- (1) a channel-vertex correction:
 δm for “quark”, $-\delta m$ for “conjugate-quark”, and 0 for mixed.
- (2) a sum of rainbow diagrams

each of which is shown in Fig. 4.3. Here the extra diagrammatic complications stem from the fact that two V “gluon” lines couple to either the “quark” or the “conjugate-quark” lines through the new vertex (see Fig. 4.2).

$$\begin{aligned}
\Sigma_1 &= \underbrace{\text{diagram 1}}_G + \underbrace{\text{diagram 2} + \text{diagram 3} + \text{diagram 4}}_{mF_{qq}} + \dots \\
&\equiv \text{diagram 1} + \text{diagram 2} \\
\Sigma_4 &= \text{diagram 3} + \text{diagram 4} \\
\Sigma_2 &= \text{diagram 5} + \text{diagram 6}
\end{aligned}$$

Fig. 4.3. Self-energy equations for the random scattering model.

The self-energy equations are explicitly given by ($G = G_{qq}$, $\bar{G} = G_{\bar{q}\bar{q}}$)

$$\begin{aligned}
\Sigma_1 &= G + mF_{qq}, \\
\Sigma_4 &= \bar{G} + mF_{\bar{q}\bar{q}}, \\
\Sigma_2 &= G_{q\bar{q}} + mF_{q\bar{q}}, \\
\Sigma_3 &= G_{\bar{q}q} + mF_{\bar{q}q}
\end{aligned} \tag{4.31}$$

where $G = (\bar{z} - \Sigma_4)/det$, $G_{q\bar{q}} = (\Sigma_2 - \lambda)/det$, etc., with $det = (z - \Sigma_1)(\bar{z} - \Sigma_4) - (\lambda - \Sigma_2)^2$. The equations for the F 's are just the generating (“Lippmann-Schwinger”) equations for the rainbow graphs, that is (see Fig. 4.4)

$$\begin{aligned}
F_{qq} &= \delta + \delta G F_{qq} + \delta G_{q\bar{q}} F_{q\bar{q}}, \\
F_{\bar{q}\bar{q}} &= -\delta - \delta \bar{G} F_{\bar{q}\bar{q}} - \delta G_{q\bar{q}} F_{q\bar{q}}, \\
F_{q\bar{q}} &= -\delta \bar{G} F_{q\bar{q}} - \delta G_{q\bar{q}} F_{qq}, \\
F_{\bar{q}q} &= \delta G_{q\bar{q}} F_{\bar{q}\bar{q}} + \delta G F_{\bar{q}q}.
\end{aligned} \tag{4.32}$$

One may solve for $F_{q\bar{q}}$ to obtain

$$F_{q\bar{q}} = \frac{-\delta^2 G_{q\bar{q}}}{denom}. \quad (4.33)$$

The equation for the mixed self-energy $\Sigma_2 \neq 0$ now gives

$$det = 1 - \frac{\delta^2 m}{denom} \quad (4.34)$$

where $denom$ is

$$denom = 1 + \delta(\bar{G} - G) - \frac{\delta^2}{det}. \quad (4.35)$$

The figure shows three Lippmann-Schwinger equations for F 's. Each equation is represented by a diagrammatic equation where a thick line with external legs is equal to a sum of diagrams. The first diagram in each sum is a simple thick line with external legs. The second and third diagrams are thick lines with a loop on top, where the loop contains a thin line with a vertex. The external legs are labeled with q , \bar{q} , and G .

Fig. 4.4. “Lippmann-Schwinger” equations for F 's.

The way to proceed now is as follows. One can write an equivalent generating equations for $F_{\bar{q}q}$ by adding the graphs on the “quark” side. This shows that $F_{q\bar{q}} = F_{\bar{q}q}$. This in conjunction with (4.34) gives the relation

$$F_{qq} + F_{\bar{q}\bar{q}} = \frac{1}{m}(G + \bar{G})(1 - det). \quad (4.36)$$

Inserting this into the self-energy equations one obtains

$$G + \bar{G} = x \quad (4.37)$$

Re-expressing $F_{\bar{q}\bar{q}}$ by $F_{q\bar{q}}$ in the appropriate self-energy equations and using (4.34) one obtains

$$\bar{z} - G det + \delta\bar{z}\bar{G} = \delta(1 - m) + \bar{G}(1 + \delta x) - \delta/det. \quad (4.38)$$

Eliminating \bar{G} , one solves this in conjunction with (4.34) treated as an equation for the determinant det :

$$[1 + \delta(x - 2G) - \delta^2/det] det = 1 + \delta(x - 2G) - \delta^2/det - \delta^2 m. \quad (4.39)$$

The final result (after changing δ into $-i\gamma$) is

$$G(z, \bar{z}) = \frac{x}{2} + \frac{i}{2} \left[\frac{1}{\gamma} + \frac{m}{y} + \frac{\gamma}{1 - \gamma y} \right]. \quad (4.40)$$

This result was first derived by Haake, Sommers and coworkers using the replica method [25], and the supersymmetric method [26].

Before closing this section we would like to mention briefly the connection of our diagrammatical approach to the mathematical concepts of free random variables [13,27]. For applications of free random variables to various physical problems see e.g. [28–32]. With the compact notations

$$\begin{aligned} \Sigma &= \begin{pmatrix} \Sigma_1 & \Sigma_2 \\ \Sigma_3 & \Sigma_4 \end{pmatrix} & \mathbf{F} &= \begin{pmatrix} F_{qq} & F_{q\bar{q}} \\ F_{\bar{q}q} & F_{\bar{q}\bar{q}} \end{pmatrix} \\ \mathcal{G} &= \begin{pmatrix} G_{qq} & G_{q\bar{q}} \\ G_{\bar{q}q} & G_{\bar{q}\bar{q}} \end{pmatrix} & \hat{\delta} &= \begin{pmatrix} \delta & 0 \\ 0 & -\delta \end{pmatrix} \end{aligned} \quad (4.41)$$

the equations (4.31) and (4.32) could be rewritten in the form

$$\begin{aligned} \Sigma &= \mathcal{G} + m\mathbf{F}, \\ \mathbf{F} &= \hat{\delta} + \hat{\delta}\mathcal{G}\mathbf{F}. \end{aligned} \quad (4.42)$$

Solving for the matrix Σ we get

$$\Sigma = \mathcal{G} + m(1 - \hat{\delta}\mathcal{G})^{-1}\hat{\delta} \quad (4.43)$$

Introducing the *generalized* Blue's function [33] (an extension of Zee's approach [31] to nonhermitean ensembles), as 2×2 matrix valued function defined by

$$\mathcal{B}(\mathcal{G}) = \mathcal{Z} = \begin{pmatrix} z & \lambda \\ \lambda & \bar{z} \end{pmatrix} \quad (4.44)$$

with $\lambda \rightarrow 0$, we see that $\Sigma = \mathcal{B}(\mathcal{G}) - \mathcal{G}^{-1}$. Therefore

$$\mathcal{B}(\mathcal{G}) = \mathcal{G} + \mathcal{G}^{-1} + m(1 - \hat{\delta}\mathcal{G})^{-1}\hat{\delta} \quad (4.45)$$

in which we recognize the generalized addition law postulated in [33], with generalized Gaussian Blue's function

$$\mathcal{B}_{gauss}(\mathcal{A}) = \frac{1}{\mathcal{A}} + \mathcal{A} \quad (4.46)$$

and generalized Blue's function for the random scattering part of the Hamiltonian form

$$\mathcal{B}_{-i\gamma V V^\dagger}(\mathcal{A}) = m(1 - \hat{\delta}\mathcal{A})^{-1}\hat{\delta} + \frac{1}{\mathcal{A}} \quad (4.47)$$

with

$$\hat{\delta} = \begin{pmatrix} i\gamma & 0 \\ 0 & -i\gamma \end{pmatrix}. \quad (4.48)$$

This completes the diagrammatic proof of the result announced already in our earlier work [33].

5 Two-Point Functions

To probe the character of the correlations between the eigenvalues of non-hermitean random matrices, either on their holomorphic or nonholomorphic supports, it is relevant to investigate two-point functions. A measure of the breaking of holomorphic symmetry in the eigenvalue distribution is given by the connected two-point function or correlator

$$N^2 G_c(z, \bar{z}) = \left\langle \left| \text{tr} \frac{1}{z - D - \mathcal{H}} \right|^2 \right\rangle_c \quad (5.1)$$

where the z and \bar{z} content of the averaging is probed simultaneously. In [34] the correlation function (5.1) was shown to diverge precisely on the nonholomorphic support of the eigenvalue distribution, indicating an accumulation in the eigenvalue density. In the conventional language of “quarks” and “gluons”, (5.1) is just the correlation function between “quarks” and their “conjugates”. A divergence in (5.1) in the z -plane reflects large fluctuations between the

eigenvalues of the nonhermitean operators on finite z -supports, hence their “condensation”.

It was shown in [10] and [35] that for hermitean matrices (with $\bar{z} \rightarrow w$) the fluctuations in connected and smoothed two-point functions satisfy the general lore of macroscopic universality. This means that all smoothed correlation functions are universal and could be classified by the support of the spectral densities, independently of the specifics of the random ensemble and genera in the topological expansion (see [36] for a recent discussion). In this section we will evaluate a number of two-point functions for random but nonhermitean ensembles on both their holomorphic and nonholomorphic supports. We confirm that the general lore of macroscopic universality extends to the nonhermitean case as well.

The concept of smoothed correlation functions will become manifest when comparing to numerical calculations. Indeed, when correlating $N \times N$ matrices at finite eigenvalue-separations, oscillations are expected due to the occurrence of a large number of eigenvalues. The correlation functions produced in the $1/N$ analysis are smoothed. Unsmoothed correlation functions are of interest for the studies of spectral form factors in the crossover region [37]. They will not be discussed here.

5.1 Notations

To establish the notations for the two-point correlators, we follow [35] and define the two-point connected (c) correlator for GUE,

$$\begin{aligned} G_c(z, w) &= \left\langle \frac{1}{N} \text{tr} \frac{1}{z - \mathcal{H}} \frac{1}{N} \text{tr} \frac{1}{w - \mathcal{H}} \right\rangle_c \\ &= \partial_z \partial_w \left\langle \frac{1}{N} \text{tr} \log(z - \mathcal{H}) \frac{1}{N} \text{tr} \log(w - \mathcal{H}) \right\rangle_c. \end{aligned} \quad (5.2)$$

Expansion of the logarithms yields

$$G_c(z, w) = \partial_z \partial_w \sum_{n=1}^{\infty} \sum_{m=1}^{\infty} \frac{1}{z^n w^m} \left\langle \frac{1}{Nn} \text{tr} \mathcal{H}^n \frac{1}{Nm} \text{tr} \mathcal{H}^m \right\rangle_c. \quad (5.3)$$

Let us first consider $n = m$. The graphs in this case are represented by the wheel diagram (Fig. 5.1a), where the rungs of the wheel are given by the “gluon” propagator from Fig. 2.1. The diagram splits into n disconnected sectors, corresponding to the fact that $\langle \text{tr} \mathcal{H}^n \text{tr} \mathcal{H}^n \rangle = n$. Resumming the

diagonal terms give to

$$N^2 G_c(z, w) = -\partial_z \partial_w \log\left(1 - \frac{1}{zw}\right). \quad (5.4)$$

All the remaining (planar) diagrams are rainbow-like (see Fig. 2.2) and correspond to dressing the bare “quark” propagators, i.e. $1/z \rightarrow G(z)$. The result is

$$N^2 G_c(z, w) = -\partial_z \partial_w \log[1 - G(z)G(w)]. \quad (5.5)$$

The two-point correlator follows functionally from the one-point correlator. Such a relation for the case of Gaussian ensemble was already noted in [38] prior to the universality arguments.

This result can be further reduced [10,35], to show that the two-point correlator depends only on the end-points of the spectral density irrespective of the choice of the weight. Since the smoothed correlation function between the eigenvalues follow from (5.5), it reflects on correlations between eigenvalues separated by N in the spectrum. Its generic form reflects on macroscopic universality in the eigenvalue correlations. This is to be contrasted with microscopic universality which is a statement about the correlations between eigenvalues one-level spacing apart in the spectrum [2].

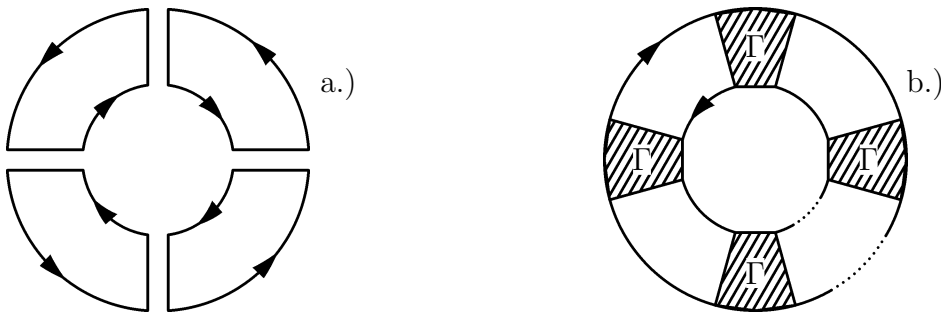


Fig. 5.1. Sample wheel diagram ($n = 4$) for the two-point correlators (GUE), (a) and generalized wheel diagram with kernel Γ (b).

5.2 Ginibre-Girko Correlator

In this section we show how to generalize (5.5) to the nonholomorphic region of complex and random matrices. We begin our discussion with the simplest case $(H_1 + iH_2)/\sqrt{2}$, where H_1 and H_2 are random hermitean Gaussians. The essential difference between this case and the case discussed above is that the “quark” propagators do not commute, and care must be taken with respect to their ordering.

The sectors of the wheel (kernel, denoted by Γ) correspond to the “two-quark” irreducible scattering amplitude. In our case it is not 1 (like in the hermitean Gaussian case) but a tensor product in “isospin” space

$$\Gamma^{f_2 f_3; g_2 g_3} = \begin{pmatrix} \mathbf{1} & 0 \\ 0 & 0 \end{pmatrix}_{f_2 f_3} \otimes \begin{pmatrix} 0 & 0 \\ 0 & \mathbf{1} \end{pmatrix}_{g_2 g_3} + \begin{pmatrix} 0 & 0 \\ 0 & \mathbf{1} \end{pmatrix}_{f_2 f_3} \otimes \begin{pmatrix} \mathbf{1} & 0 \\ 0 & 0 \end{pmatrix}_{g_2 g_3}. \quad (5.6)$$

The two terms correspond to the “gluon” amplitudes of Fig. 3.1b and 3.1c, respectively. This particular form becomes transparent in Fig. 5.2.

$$= \mathcal{G}_{f_1 f_2} \otimes \mathcal{G}_{g_1 g_2}^T \Gamma^{f_2 f_3; g_2 g_3}$$

Fig. 5.2. Two-point kernel with $f, g = q, \bar{q}$.

The factors

$$\frac{1}{zw} \quad (5.7)$$

get transformed (after “dressing”) into

$$\mathcal{G}(z) \otimes \mathcal{G}^T(w). \quad (5.8)$$

Here $\mathcal{G}(z)$ and $\mathcal{G}(w)$ are the resolvents discussed in section 4.1 with $\tau = 0$. Transposition keeps track of the “flow” of indices.

Another generalization deals with the treatment of the derivatives. Now the logarithm is not a holomorphic functions so we must treat ∂_z as

$$\partial_z = \frac{1}{2}(\partial_x - i\partial_y) \quad (5.9)$$

where $z = x + iy$ and

$$\partial_{\bar{w}} = \frac{1}{2}(\partial_u + i\partial_v) \quad (5.10)$$

where $w = u + iv$. Note that in order to obtain $G(z, \bar{z})$ we *cannot* write the derivatives as $\partial_z \partial_{\bar{z}}$ but rather $\partial_z \partial_{\bar{w}}$ and set $\bar{w} = \bar{z}$ at the end of the calculation.

The choice of “isospin” in the lower fermion loop is done by choosing the appropriate derivative ∂_w for the “quark” and $\partial_{\bar{w}}$ for the “conjugate-quark”. As

in [11], two distinct contributions may be identified. First, when the derivatives (bullets) act on the exposed or hidden Γ lines within the same sector of the wheel, as shown in Fig. 5.3. Second, when the derivatives act on different sectors as shown in Fig. 5.4.

$$\partial_1 \partial_2 \left(\begin{array}{c} 1 \\ \text{---} \text{---} \text{---} \\ \text{---} \text{---} \text{---} \\ 2 \end{array} \right) = \begin{array}{c} \bullet \\ \text{---} \text{---} \text{---} \\ \text{---} \text{---} \text{---} \\ \bullet \end{array} + \begin{array}{c} \bullet \\ \text{---} \text{---} \text{---} \\ \text{---} \text{---} \text{---} \\ \bullet \end{array} + \begin{array}{c} \text{---} \text{---} \text{---} \\ \bullet \text{---} \text{---} \text{---} \\ \text{---} \text{---} \text{---} \\ \bullet \end{array} + \begin{array}{c} \text{---} \text{---} \text{---} \\ \bullet \text{---} \text{---} \text{---} \\ \text{---} \text{---} \text{---} \\ \bullet \end{array} = \partial_1 \partial_2 (\mathcal{G}_1 \otimes \mathcal{G}_2^T \Gamma)$$

Fig. 5.3. Derivatives acting within the same sector of Γ in the wheel.

$$\begin{aligned} \partial_1 \partial_2 \left(\begin{array}{c} 1 \\ \text{---} \text{---} \text{---} \text{---} \\ \text{---} \text{---} \text{---} \text{---} \\ 2 \end{array} \right) &= \left(\begin{array}{c} \text{---} \text{---} \text{---} \\ \bullet \text{---} \text{---} \text{---} \\ \text{---} \text{---} \text{---} \\ \bullet \end{array} + \begin{array}{c} \text{---} \text{---} \text{---} \\ \text{---} \text{---} \text{---} \\ \bullet \text{---} \text{---} \text{---} \\ \bullet \end{array} \right) \cdot \left(\begin{array}{c} \bullet \\ \text{---} \text{---} \text{---} \\ \text{---} \text{---} \text{---} \\ \bullet \end{array} + \begin{array}{c} \bullet \\ \text{---} \text{---} \text{---} \\ \text{---} \text{---} \text{---} \\ \bullet \end{array} \right) \\ &= \dots \partial_1 (\mathcal{G}_1 \otimes \mathcal{G}_2^T \Gamma) \dots \partial_2 (\mathcal{G}_1 \otimes \mathcal{G}_2^T \Gamma) \end{aligned}$$

Fig. 5.4. Derivatives (bullets) acting on two different sectors of Γ .

Finally, we have

$$\begin{aligned} N^2 G_c(z, w) &= \text{tr}_{q\bar{q}} \left(\frac{1}{1 - \mathcal{G}_1 \otimes \mathcal{G}_2^T \Gamma} \partial_z \partial_w (\mathcal{G}_1 \otimes \mathcal{G}_2^T \Gamma) \right. \\ &\quad + \frac{1}{1 - \mathcal{G}_1 \otimes \mathcal{G}_2^T \Gamma} \partial_z (\mathcal{G}_1 \otimes \mathcal{G}_2^T \Gamma) \\ &\quad \left. \times \frac{1}{1 - \mathcal{G}_1 \otimes \mathcal{G}_2^T \Gamma} \partial_w (\mathcal{G}_1 \otimes \mathcal{G}_2^T \Gamma) \right) \end{aligned} \quad (5.11)$$

as an apparent generalization of the Brézin-Hikami-Zee formalism. The denominators in the above formula come from the fact that the dotted lines in Figs. 5.3, 5.4 could represent $0, 1, 2, \dots, \infty$ sectors Γ of the wheel (see Fig. 5.1b) and have to be resummed. The last result may be rewritten as

$$N^2 G_c(z, w) = -\partial_z \partial_w \text{tr}_{q\bar{q}} \log (1 - \mathcal{G}_1 \otimes \mathcal{G}_2^T \Gamma). \quad (5.12)$$

Here the logarithm is understood as a power series expansion. The operator $\mathcal{G}_1 \otimes \mathcal{G}_2^T \Gamma$ is a tensor product of 2×2 matrices. One can rewrite it as an ordinary 4×4 matrix. The trace $\text{tr}_{q\bar{q}}$ becomes an ordinary matrix trace. This allows the following reformulation

$$N^2 G_c(z, w) = -\partial_z \partial_w \log \det(1 - \mathcal{G}_1 \otimes \mathcal{G}_2^T \Gamma). \quad (5.13)$$

Using the explicit expressions for the Ginibre-Girko resolvents (4.1)

$$\mathcal{G}_1 = \begin{pmatrix} \bar{z} & g_z \\ g_z & z \end{pmatrix}, \quad (5.14)$$

$$\mathcal{G}_2 = \begin{pmatrix} \bar{w} & g_w \\ g_w & w \end{pmatrix} \quad (5.15)$$

where $g_z^2 = |z|^2 - 1$, the operator $\mathcal{G}_1 \otimes \mathcal{G}_2^T \Gamma$ can be evaluated to

$$\left[\begin{pmatrix} \bar{z} & 0 \\ g_z & 0 \end{pmatrix} \otimes \begin{pmatrix} 0 & g_w \\ 0 & w \end{pmatrix} + \begin{pmatrix} 0 & g_z \\ 0 & z \end{pmatrix} \otimes \begin{pmatrix} \bar{w} & 0 \\ g_w & 0 \end{pmatrix} \right]. \quad (5.16)$$

In a 4 by 4 matrix notation $\mathcal{G}_1 \otimes \mathcal{G}_2^T \Gamma$ is

$$\mathcal{G}_1 \otimes \mathcal{G}_2^T \Gamma = \begin{pmatrix} 0 & \bar{z}g_w & g_z\bar{w} & 0 \\ 0 & \bar{z}w & g_zg_w & 0 \\ 0 & g_zg_w & z\bar{w} & 0 \\ 0 & g_zw & zg_w & 0 \end{pmatrix}. \quad (5.17)$$

The determinant of $1 - \mathcal{G}_1 \otimes \mathcal{G}_2^T \Gamma$ gives $|z - w|^2$, so

$$N^2 G_{qq}(z, w) = \frac{-1}{(w - z)^2}. \quad (5.18)$$

$$N^2 G_{q\bar{q}}(z, w) = 0. \quad (5.19)$$

5.3 Elliptic Correlator

We consider now the general case of subsection 4.1. In this case, there is an extra contribution to the Ginibre-Girko diagrams, due to the τ terms in the “gluonic” propagator. In terms of graphs, another diagram may contribute to Γ with a penalty factor τ (see Fig. 3.1e and 3.1h). As a result,

$$\begin{aligned} \Gamma = & \begin{pmatrix} \mathbf{1} & 0 \\ 0 & 0 \end{pmatrix} \otimes \begin{pmatrix} 0 & 0 \\ 0 & \mathbf{1} \end{pmatrix} + \begin{pmatrix} 0 & 0 \\ 0 & \mathbf{1} \end{pmatrix} \otimes \begin{pmatrix} \mathbf{1} & 0 \\ 0 & 0 \end{pmatrix} \\ & + \tau \begin{pmatrix} \mathbf{1} & 0 \\ 0 & 0 \end{pmatrix} \otimes \begin{pmatrix} \mathbf{1} & 0 \\ 0 & 0 \end{pmatrix} + \tau \begin{pmatrix} 0 & 0 \\ 0 & \mathbf{1} \end{pmatrix} \otimes \begin{pmatrix} 0 & 0 \\ 0 & \mathbf{1} \end{pmatrix}. \end{aligned} \quad (5.20)$$

The rest of the calculation follows the Ginibre-Girko case, with the resolvents for the elliptic case as in section 4.1

$$\mathcal{G}_1 = \frac{1}{1-\tau^2} \begin{pmatrix} \bar{z} - \tau z & g_z \\ g_z & z - \tau \bar{z} \end{pmatrix} \quad (5.21)$$

$$\mathcal{G}_2 = \frac{1}{1-\tau^2} \begin{pmatrix} \bar{w} - \tau w & g_w \\ g_w & w - \tau \bar{w} \end{pmatrix} \quad (5.22)$$

with $g_z^2 = |z|^2(1-\tau)^2 - \tau(z+\bar{z})^2 - (1-\tau^2)^2$. After defining $c_\tau = (1-\tau^2)^{-2}$, $z_\tau = z - \tau\bar{z}$, $w_\tau = w - \tau\bar{w}$, we have

$$N^2 G_c(z, \bar{w}) = -\partial_z \partial_{\bar{w}} \log \det \mathcal{L} \quad (5.23)$$

where \mathcal{L} is given explicitly by

$$\mathcal{L} = \frac{1}{c_\tau} \begin{pmatrix} c_\tau - \tau \bar{z}_\tau \bar{w}_\tau & -\bar{z}_\tau g_w & -g_z \bar{w}_\tau & -\tau g_z g_w \\ -\tau \bar{z}_\tau g_w & c_\tau - \bar{z}_\tau w_\tau & -g_z g_w & -\tau g_z w_\tau \\ -\tau g_z \bar{w}_\tau & -g_z g_w & c_\tau - z_\tau \bar{w}_\tau & -\tau z_\tau g_w \\ -\tau g_z g_w & -g_z w_\tau w & -z_\tau g_w & c_\tau - \tau z_\tau w_\tau \end{pmatrix}. \quad (5.24)$$

After some remarkable cancellations, the determinant \mathcal{L} is again simply $|z-w|^2$, giving the correlators (5.18–5.19).

Figure 5.5 compares the analytical results (5.18) (solid lines) for the “quark-quark” correlator, to the numerical calculations (dashed lines) using an ensemble of 50000 matrices of size 100×100 for $\tau = 0.5$ (real/major axis is 1.5, imaginary/minor is 0.5). The figures on the left are parameterized by $z = t$, $w = t/\sqrt{2}(1+i)$, while those on the right are parameterized by $z = t/\sqrt{2}(1+i)$, $w = it$. In Fig. 5.6 we show the analytical result (thick solid line) for the “quark-conjugate-quark” correlator (5.19) versus the numerical calculations for different matrix sizes $N = 50, 100, 200$. The peak around zero in the numerical calculations is proportional to N , while its width decreases with larger matrices, approaching zero in the large N limit. Our analytical evaluation of the correlators disregard delta-functions.

Let us now investigate the case of *real* asymmetric matrices defined by (3.5). When the ‘twisted’ propagator

$$\langle M_{ij} M_{ij} \rangle = \frac{1}{N} \quad (5.25)$$

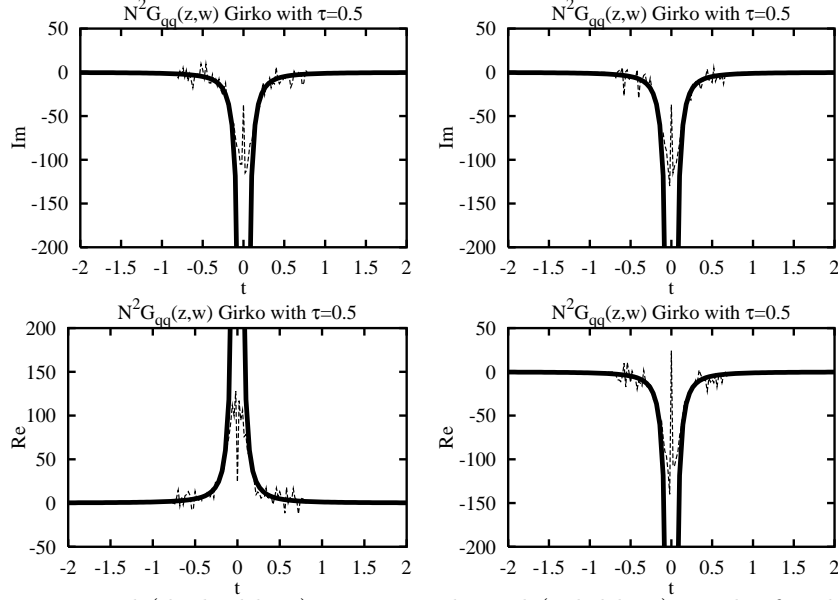


Fig. 5.5. Numerical (dashed line) versus analytical (solid line) results for the elliptic correlators from GUE (see text).

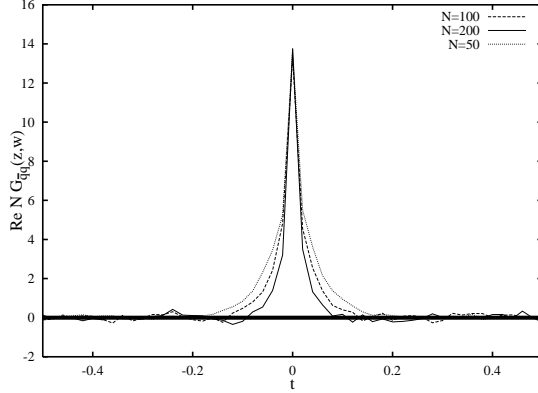


Fig. 5.6. Same as Fig. 5.5 but for the “quark-conjugate-quark” correlator divided by N . The analytical result (5.19) is zero in this region.

couples at both ends to the same “quark” (as is the case for the self-energy) it gives a subleading contribution in $1/N$ (see Fig. 4.1). But in the calculation of the correlator it may couple to two different “quark” loops giving a planar contribution. Now it joins “quarks” of the same species. Similar arguments apply for the ‘ τ ’-propagator which joins “quarks” and “conjugate-quarks”. Diagrammatically we observe that the ‘twisted’ propagators and the ones considered earlier cannot mix in the planar limit so we must add the two resummed contributions separately — the one calculated earlier and the twisted one given by

$$-\partial_1 \partial_2 \log \det(\mathbf{1} - \mathcal{G}_1(z) \otimes \mathcal{G}_2^T(w) \cdot \Gamma_{twisted}) \quad (5.26)$$

where $\Gamma_{twisted}$ is given by the expression obtained from (5.20) after interchanging 1 and τ :

$$\begin{aligned} \Gamma_{twisted} = & \begin{pmatrix} \mathbf{1} & 0 \\ 0 & 0 \end{pmatrix} \otimes \begin{pmatrix} \mathbf{1} & 0 \\ 0 & 0 \end{pmatrix} + \begin{pmatrix} 0 & 0 \\ 0 & \mathbf{1} \end{pmatrix} \otimes \begin{pmatrix} 0 & 0 \\ 0 & \mathbf{1} \end{pmatrix} \\ & + \tau \begin{pmatrix} \mathbf{1} & 0 \\ 0 & 0 \end{pmatrix} \otimes \begin{pmatrix} 0 & 0 \\ 0 & \mathbf{1} \end{pmatrix} + \tau \begin{pmatrix} 0 & 0 \\ 0 & \mathbf{1} \end{pmatrix} \otimes \begin{pmatrix} \mathbf{1} & 0 \\ 0 & 0 \end{pmatrix}. \end{aligned} \quad (5.27)$$

Here the terms correspond respectively to the ‘‘gluonic’’ amplitudes in Fig. 3.1a, 3.1d, 3.1f and 3.1g. The determinant is now given by

$$const \cdot (w - \bar{z})(\bar{w} - z). \quad (5.28)$$

This leads to correlators of the form:

$$N^2 G_{qq}(z, w) = \frac{-1}{(w - z)^2}, \quad (5.29)$$

$$N^2 G_{q\bar{q}}(z, \bar{w}) = \frac{-1}{(\bar{w} - z)^2}. \quad (5.30)$$

Note that these are different expressions than in the complex case, although the Green’s functions are identical in both cases.

5.4 Chiral Correlator I (Holomorphic Region)

In the nonhermitean (chiral) case the correlator in the *outside* region is calculated using the same arguments as above. In the outside, the resolvents are holomorphic, hence we may consider the derivatives as acting on analytical functions. The amplitude Γ reads in this case

$$\Gamma = \begin{pmatrix} 0 & \mathbf{1} \\ 0 & 0 \end{pmatrix}_{ab} \otimes \begin{pmatrix} 0 & \mathbf{1} \\ 0 & 0 \end{pmatrix}_{cd} + \begin{pmatrix} 0 & 0 \\ \mathbf{1} & 0 \end{pmatrix}_{ab} \otimes \begin{pmatrix} 0 & 0 \\ \mathbf{1} & 0 \end{pmatrix}_{cd} \quad (5.31)$$

where ab are the ‘‘quark’’ indices and cd are the ‘‘conjugate-quark’’ indices. Note that the kernel is rewritten in the chiral basis, i.e. the indices a, b, c and d run from 1 to $2N$. The correlator reads

$$N^2 G_c(z, \bar{z}) = -\frac{1}{4} \partial_z \partial_{\bar{z}} \log \det(1 - \mathcal{G}_{qq}(z) \otimes \mathcal{G}_{q\bar{q}}^T(z) \Gamma) \quad (5.32)$$

From the definition of \mathcal{G} in (4.20) we see, that in the holomorphic case ($\Sigma_2 = \Sigma_3 = 0$ and $\Sigma_1 = G$) the \mathcal{G}_{qq} component (after performing the trivial tracing of the diagonal $N \times N$ blocks) is simply

$$\mathcal{G}_{qq} = \begin{pmatrix} z - \Sigma_1 & \mu \\ -\mu & z - \Sigma_1 \end{pmatrix}^{-1} \quad (5.33)$$

where we used the explicit chiral structure (4.19). Performing the inversion we arrive at

$$\mathcal{G}_{qq} = \frac{1}{\det} \begin{pmatrix} z - G & -\mu \\ \mu & z - G \end{pmatrix}, \quad (5.34)$$

$$\mathcal{G}_{\bar{q}\bar{q}}^T = \frac{1}{\overline{\det}} \begin{pmatrix} \bar{z} - \bar{G} & -\mu \\ \mu & \bar{z} - \bar{G} \end{pmatrix} \quad (5.35)$$

with the determinants given by

$$\det = (z - G)^2 + \mu^2, \quad \overline{\det} = (\bar{z} - \bar{G})^2 + \mu^2 \quad (5.36)$$

with G being the solution of Pastur equation (4.28) and \bar{G} is just the complex conjugate of G . Now the operator $\mathcal{G}_1 \otimes \mathcal{G}_2^T \Gamma$ reads

$$\frac{1}{|\det|^2} \left[\begin{pmatrix} 0 & z - G \\ 0 & \mu \end{pmatrix} \otimes \begin{pmatrix} 0 & \bar{z} - \bar{G} \\ 0 & \mu \end{pmatrix} + \begin{pmatrix} -\mu & 0 \\ z - G & 0 \end{pmatrix} \otimes \begin{pmatrix} -\mu & 0 \\ \bar{z} - \bar{G} & 0 \end{pmatrix} \right]. \quad (5.37)$$

or in 4×4 form

$$\frac{1}{D} \cdot \begin{pmatrix} \mu^2 & 0 & 0 & |z - G|^2 \\ -\mu(\bar{z} - \bar{G}) & 0 & 0 & \mu(z - G) \\ -\mu(z - G) & 0 & 0 & \mu(\bar{z} - \bar{G}) \\ |z - G|^2 & 0 & 0 & \mu^2 \end{pmatrix}, \quad (5.38)$$

with

$$D \equiv |\det|^2 = \frac{|z - G|^2}{|G|^2}. \quad (5.39)$$

where holomorphic G is the appropriate branch of (4.28) rewritten in the form $G[(z - G)^2 + \mu^2] = z - G$. The determinant of $1 - \mathcal{G}_1 \otimes \mathcal{G}_2^T \Gamma$ gives

$$\frac{(D - \mu^2)^2 - |z - G|^4}{D^2} \quad (5.40)$$

The zero of the determinant in (5.32) occurs for $(D - \mu^2) = |z - G|^2$, that is

$$|z - G|^2(1 - |G|^2) - \mu^2|G|^2 = 0 \quad (5.41)$$

as quoted in [34]. In the case $\mu = 0$ (and $\bar{z} = w$), the determinant in (5.32) is simply $(1 - G^2(z)G^2(w))$ (chiral) as opposed to $(1 - G(z)G(w))$ (non-chiral). As a result, for $w = z$ and $\mu = 0$, (5.32) is

$$N^2 G(z, z) = 1/(z^2(z^2 - 4)^2) \quad (5.42)$$

which coincides with (5.5) in [39]. For small z , the behavior $G(z, z) \sim 1/z^2$ reflects the exchange of two “massless” modes for $z = im \rightarrow 0$.

The numerical results for the chiral correlator versus the present analytical results are shown in Fig. 5.7. The dashed line is obtained from a numerical simulation of 200 100×100 matrices at $\mu^2 = 2$, while the solid line follows from (5.32). The dashed region indicates the extent of the nonholomorphic region for this choice of $\mu^2 = 2$, over which the result (5.32) no longer holds.

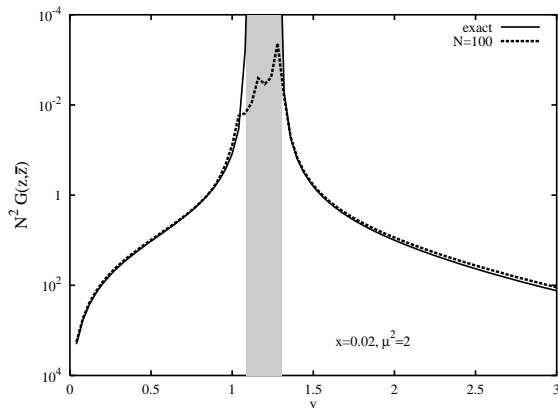


Fig. 5.7. Numerical (dashed) versus analytical (solid line) results for the chiral correlator I. The nonholomorphic region is shown dashed.

5.5 Chiral Correlator II (Non-Holomorphic Region)

As an extension of this construction we consider the case of a nonhermitean deterministic matrix plus a hermitean chiral random matrix. The extension

amounts to adding an “isospin” index to the resolvents which are now 4×4 matrices (2 “isospin” + 2 chirality). The original 4×4 matrix $\mathcal{G}_{qq}(z) \otimes \mathcal{G}_{\bar{q}\bar{q}}^T(w)\Gamma$ is now changed into a 16×16 matrix (each factor in the tensor product is now 4×4 so the tensor product has dimension 16). The matrix $\mathcal{G}(z) \otimes \mathcal{G}^T(w)\Gamma$ is of the form

$$\begin{pmatrix} \mathcal{G}_{qq} \otimes \mathcal{G}_{qq}^T \Gamma & \mathcal{G}_{qq} \otimes \mathcal{G}_{\bar{q}\bar{q}}^T \Gamma & \mathcal{G}_{q\bar{q}} \otimes \mathcal{G}_{qq}^T \Gamma & \mathcal{G}_{q\bar{q}} \otimes \mathcal{G}_{\bar{q}\bar{q}}^T \Gamma \\ \mathcal{G}_{qq} \otimes \mathcal{G}_{\bar{q}\bar{q}}^T \Gamma & \mathcal{G}_{qq} \otimes \mathcal{G}_{\bar{q}\bar{q}}^T \Gamma & \mathcal{G}_{q\bar{q}} \otimes \mathcal{G}_{\bar{q}\bar{q}}^T \Gamma & \mathcal{G}_{q\bar{q}} \otimes \mathcal{G}_{\bar{q}\bar{q}}^T \Gamma \\ \mathcal{G}_{\bar{q}\bar{q}} \otimes \mathcal{G}_{qq}^T \Gamma & \mathcal{G}_{\bar{q}\bar{q}} \otimes \mathcal{G}_{\bar{q}\bar{q}}^T \Gamma & \mathcal{G}_{q\bar{q}} \otimes \mathcal{G}_{qq}^T \Gamma & \mathcal{G}_{q\bar{q}} \otimes \mathcal{G}_{\bar{q}\bar{q}}^T \Gamma \\ \mathcal{G}_{\bar{q}\bar{q}} \otimes \mathcal{G}_{\bar{q}\bar{q}}^T \Gamma & \mathcal{G}_{\bar{q}\bar{q}} \otimes \mathcal{G}_{\bar{q}\bar{q}}^T \Gamma & \mathcal{G}_{q\bar{q}} \otimes \mathcal{G}_{\bar{q}\bar{q}}^T \Gamma & \mathcal{G}_{q\bar{q}} \otimes \mathcal{G}_{\bar{q}\bar{q}}^T \Gamma \end{pmatrix} \quad (5.43)$$

The complexity in this case stems from the fact that in the nonholomorphic region “quarks” may turn to “conjugate-quarks” and vice-versa, with all “quark” species interacting with themselves.

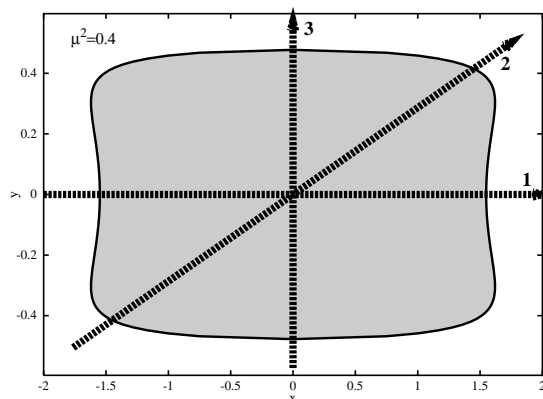


Fig. 5.8. Extent of the non-holomorphic region (shaded) for the chiral ensemble at $\mu^2 = 0.4$. The thick dashed lines indicate the paths along which the numerical correlator was evaluated.

The resolvents in (5.43) follow from the solutions presented in section 4.3. Defining $z = x + iy$, $w = u + iv$, we have

$$\begin{aligned} \mathcal{G}_{qq} &= (\bar{z} + \mu\gamma - \Sigma_4) \cdot \Delta^{-1} = \begin{pmatrix} \Sigma_1 & (\bar{z} - \Sigma_4)iy/\mu - \mu \\ -(\bar{z} - \Sigma_4)iy/\mu + \mu & \Sigma_1 \end{pmatrix}, \\ \mathcal{G}_{\bar{q}\bar{q}} &= (z - \mu\gamma - \Sigma_1) \cdot \Delta^{-1} = \begin{pmatrix} \Sigma_4 & (z - \Sigma_1)iy/\mu + \mu \\ -(z - \Sigma_1)iy/\mu - \mu & \Sigma_4 \end{pmatrix}, \\ \mathcal{G}_{q\bar{q}} &= R \cdot \Delta^{-1} = R \begin{pmatrix} 1 & iy/\mu \\ -iy/\mu & 1 \end{pmatrix} \end{aligned} \quad (5.44)$$

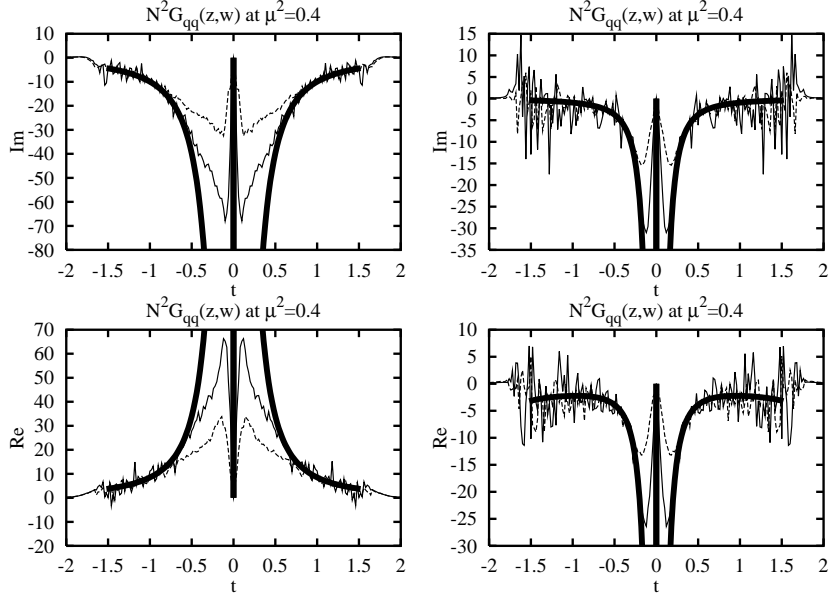


Fig. 5.9. Numerical (thin and dashed lines) versus analytical (thick solid lines) results for the chiral “quark-quark” correlators II. The correlators were evaluated along the paths shown in Fig. (5.8): $z-w=1-2$ (left), $2-3$ (right).

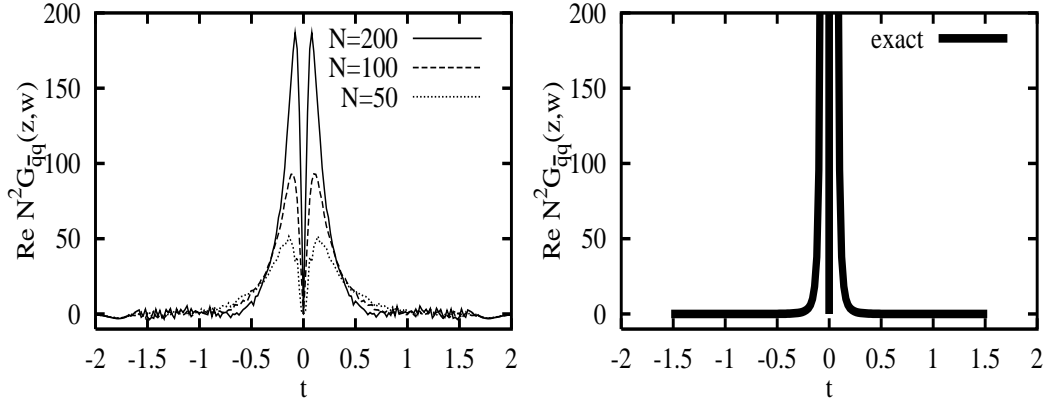


Fig. 5.10. Same as Fig. 5.9 for “quark-conjugate-quark” chiral correlator II.

where

$$(z - \Sigma_1)(\bar{z} - \Sigma_4) + \mu^2 - R^2 = \det = \frac{-\mu^2}{y^2 - \mu^2} \quad (5.45)$$

and

$$\Sigma_1 = \frac{x}{2} + iy + \frac{1}{2} \frac{iy}{y^2 - \mu^2}, \quad (5.46)$$

$$\Sigma_4 = \frac{x}{2} - iy - \frac{1}{2} \frac{iy}{y^2 - \mu^2}. \quad (5.47)$$

Using (5.44-5.47), the determinant of (5.43) viewed as a 16×16 matrix simplifies to

$$\det(1 - \mathcal{G}(z) \otimes \mathcal{G}^T(w)\Gamma) = |z-w|^2 |z+w|^2 \frac{(\mu^2 - (\mu^2 - y^2)(\mu^2 - v^2))^2 - v^2 y^2}{\mu^4} \quad (5.48)$$

We have evaluated the correlator numerically inside the nonholomorphic region. Figure 5.8 shows the island for $\mu^2 = 0.4$, and indicates the paths z and w taken during the numerical evaluation of the correlator. In Fig. 5.9 the analytical results (5.43) are compared to the numerical simulations. The thin solid line is obtained from a numerical simulation of 73000 200×200 matrices at $\mu^2 = 0.4$, the dashed line represents 75000 events of 100×100 matrices, while the thick solid line is deduced from the analytical prediction (5.43). The numerical results converge slowly to the analytical one. In Fig. 5.10, the thick solid line on the right corresponds to the analytical prediction (5.43), while the thin lines on the left are the numerical simulation using 15000 50×50 (dotted), 15000 100×100 (dashed) and 10000 200×200 matrices (solid line). The height of the numerical peak is proportional to N , diverging in the large N limit. Its width is slowly approaching the analytical one.

5.6 Scattering Correlator

Here we consider the correlator for the model discussed in section 3.4, that is

$$H - i\gamma VV^\dagger = H - \delta VV^\dagger \quad (5.49)$$

where H is random Gaussian Hermitean. The precedent discussion can be easily adapted to this case by assessing Γ the “quark-quark” scattering amplitude. In this case, the latter splits into a sum Γ^H and Γ^{VV^\dagger} . The first one is just

$$\Gamma_{f_1 f_2; g_1 g_2}^H = \delta_{f_1 f_2} \delta_{g_1 g_2} \quad (5.50)$$

where f_1, f_2 are the ingoing and respectively outgoing “quark isospin” on the upper line, while the g_i 's are the corresponding ones for the lower lines (see Fig. 5.11a). The graphs Γ^{VV^\dagger} are considerably more involved (see Fig. 5.11b) due to the fact that the V vertices always appear in pairs. Therefore they always contain an exchange of two F propagators between the “quark” lines. Note that the 1PI “quark” scattering amplitude Γ^{VV^\dagger} flips “quarks” into “conjugate-quarks” and vice-versa on the upper and the lower lines. With

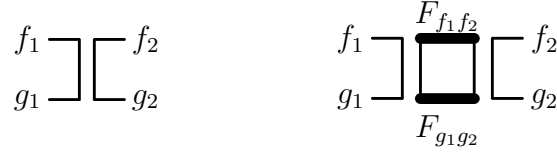


Fig. 5.11. a) Graph contributing to Γ^{VV^\dagger} (left) and b) graph contributing to Γ^H (right).

this in mind,

$$\Gamma_{f_1 f_2; g_1 g_2}^{VV^\dagger} = m \cdot F_{f_1 f_2} \cdot F_{g_1 g_2} \quad (5.51)$$

where the F 's are defined by Fig. 4.4 and the factor m comes from the interior loop of Fig. 5.11b. Hence ($z = x + iy, w = u + iv$)

$$F_{qq} = \delta(1 + \delta\overline{G})/\text{den} \quad (5.52)$$

$$F_{\overline{q}\overline{q}} = -\delta(1 - \delta G)/\text{den} \quad (5.53)$$

$$F_{q\overline{q}} = -\delta^2 G_{q\overline{q}}/\text{den} \quad (5.54)$$

where

$$\text{den} = \frac{-\gamma m}{y} \quad (5.55)$$

and

$$G_{q\overline{q}} = \sqrt{G\overline{G} - \frac{1}{1 - \gamma y}} \quad (5.56)$$

In the present model the ‘‘quark-quark’’ correlator is now

$$N^2 G_{qq}(z, w) = -\partial_z \partial_w \log \det(1 - \mathcal{G}(z) \otimes \mathcal{G}^T(w) \cdot [\Gamma^H + \Gamma^{VV^\dagger}]) \quad (5.57)$$

where the dot stands for ordinary matrix multiplication. The determinant in (5.57) may be explicitly evaluated to give

$$\det(\dots) = |z - w|^2 \frac{(1 - \gamma y)(1 - \gamma v)(m + yv) - \gamma^2 yv}{m(1 - \gamma y)^2(1 - \gamma v)^2}. \quad (5.58)$$

As in the case of the elliptic ensemble, the correlators differ depending on whether the matrices Γ and V stem from GUE or GOE ensembles. In the last case, a new set of diagrams have to be added. They are leading in GOE and subleading in GUE. We have checked that the additional contribution is the same as (5.58), resulting into an extra factor of 2 for the GOE correlators.

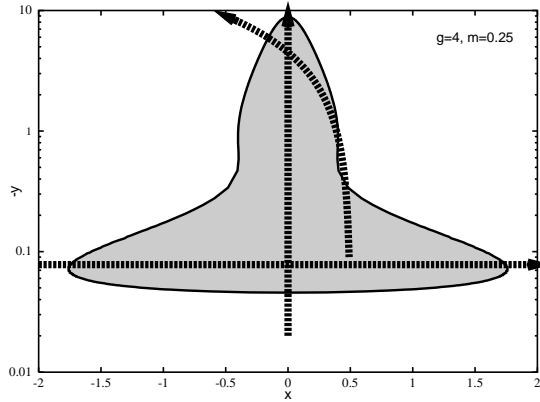


Fig. 5.12. Extent of the nonholomorphic region (shaded) for the scattering problem at $g = 4, m = 0.25$. The thick dashed lines indicate the paths along which the numerical correlator was evaluated (see below).

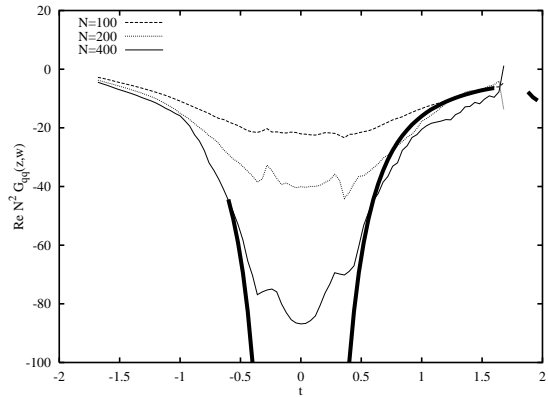


Fig. 5.13. Numerical versus analytical (thick solid lines) for the “quark-quark” correlator of the random scattering problem.

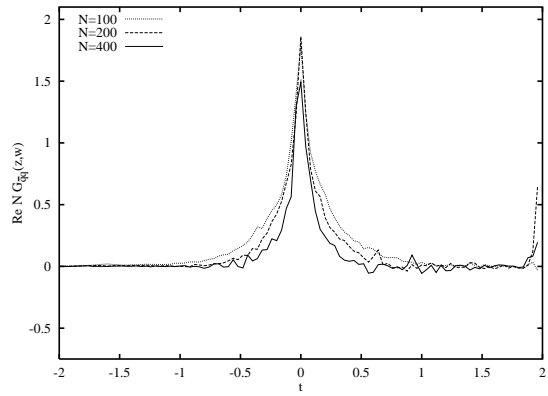


Fig. 5.14. Same as Fig. 5.13 but for the “quark-conjugate-quark” correlation function divided by N . The analytical result (5.57) is not distinguishable from zero on the plot (see text).

Figure 5.13 compares the numerical versus analytical results for random scattering correlator using GUE ensembles along the paths indicated on Fig. 5.12. The thick solid line is the analytical result (5.57), while the thin lines follow from numerical simulation of 10000 100×100 (dashed), 3000 200×200 (dotted) and 2000 400×400 matrices (solid) at $\gamma = 4$, $m = 0.25$ along the trajectory $z = 0.777t(2 + 0.2865i)$, $w = 0.2865it$. Part of the path goes outside the non-holomorphic region as shown in Fig. 5.12 and the analytical curve is missing for that values. The convergence of the numerical results to the analytical one is slow. The numerical results for the “quark-conjugate-quark” correlators are shown in Fig. 5.14. The analytical result (5.57) is not distinguishable from zero in the region shown. The large central peak is a finite size effect, as it starts to shrink for $N \sim 400$.

6 Partition Functions

From a “thermodynamical” point of view, the information carried by the one- and two-point functions is sufficient to specify the “thermodynamical” potential to order $\mathcal{O}(1/N)$ in the entire z -plane modulo isolated singularities, as we now discuss. Similar ideas were used either in the context of two-dimensional models in matter [40], or as a way to calculate next-to-leading corrections to hermitean correlators [3], exploiting the functional formalism discussed in [41].

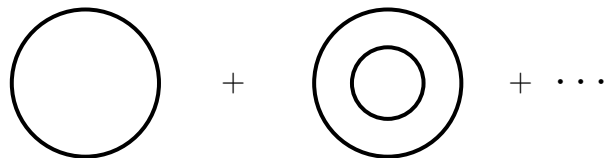


Fig. 6.1. Leading contributions to Z_N in (6.2).

Let Z_N be the partition function in the presence of an external parameter z . In the $1/N$ approximation, the diagrammatic contributions to the partition function Z_N are shown in Fig. 6.1, corresponding to

$$\log Z_N = NE_0 + E_1 + \mathcal{O}\left(\frac{1}{N}\right) \quad (6.1)$$

E_0 is the contribution of the “quark” or “conjugate quark” loop in the planar approximation, and E_1 is contribution of the “quark-quark” loop, and so on, in the same approximation. Throughout this section, we will restrict our attention to nonhermitean matrices with unitary randomness, in which case the non-planar corrections to E_0 are of order $1/N^2$.² Hence, E_0 is determined by the one-point function and E_1 by the two-point functions.

² A similar observation was made in [3], while evaluating the correction to the resolvent for hermitean GUE ensembles.

For z such that (6.1) is real, continuous and nondecreasing function of the extensive parameters [42], $\log Z_N/N$ may be identified with the “pressure” of the random matrix model. As a result, the isolated singularities in the “pressure” are just the “phase” boundaries provided that the expansion is uniform. Below we give examples where the “phase” boundary is either mean-field-driven or fluctuation-driven.

6.1 Holomorphic Z

To illustrate the above arguments, consider the partition function

$$Z_N = \langle \det(z - \mathcal{M}) \rangle = \left\langle \int d\psi d\bar{\psi} e^{-\bar{\psi}(z - \mathcal{M})\psi} \right\rangle \quad (6.2)$$

In contrast to the one- and two-point correlators discussed above, the determinant in (6.2) is not singular in the z -plane configuration by configuration. Hence, (6.2) is *a priori* holomorphic in z (minus isolated singularities).

The one- and two-point functions on their holomorphic support may be obtained from $\log Z_N$ by differentiation with respect to z . Therefore, from (6.1)

$$E_0 = \int^z dz' G(z') + const \quad (6.3)$$

or equivalently

$$E_0 = zG - \int dG z(G) + const \quad (6.4)$$

after integrating by part. Note that $z(G) = B(G)$ is just the Blue’s function [31] of G (where the Blue’s function is the functional inverse of the resolvent, i.e. $B[G(z)] = z$). The constant in E_0 is fixed by the asymptotic behavior of (6.2), that is $Z_N \sim z^N$. The planar contribution to E_1 in (6.1) follows from the “quark-quark” wheel of Fig. 6.1, that is

$$E_1 = -\frac{1}{2} \log \det(1 - \mathcal{G} \otimes \mathcal{G}^T \cdot \Gamma) \quad (6.5)$$

which can be understood by opening one of the lines in the two-point correlator (5.12): the factor 1/2 is combinatorial (two identical “quarks”) and the minus sign corresponds to decreasing the number of fermion loops by one. The derivative amputates the left out propagator after “opening” the fermionic loop. We

note that the factor $-1/2$ in (6.5) causes the “quark-quark” contribution to be overall “bosonic”³. Hence

$$Z_N = e^{NE_0} \cdot \left(\left\{ \det(1 - \mathcal{G} \otimes \mathcal{G}^T \cdot \Gamma) \right\}^{-\frac{1}{2}} + \mathcal{O}\left(\frac{1}{N}\right) \right) \quad (6.6)$$

In contrast to the “quark” contribution, the “bosonic” contribution is not extensive in N , since in random matrix models N is like “color” not “space”. The “bosonic” contribution is dwarfed by the “quark” contribution ($1 : N$) [43]. Both E_0 and E_1 are simple functions of the resolvent on a specific branch as we will show in the examples below. When the “quark-quark” contribution (pre-exponent) to (6.6) does not vanish in the z -plane, the singularities of Z_N are those of the “quark” contribution in E_0 in large N . Such singularities are mean-field-driven. Otherwise, they are fluctuation-driven.

We note that the partition function Z_N through (6.6) exhibits an essential singularity in $1/N$ as expected from thermodynamical arguments. Assuming that the expansion for $\log Z_N/N$ is uniform, then $\log Z_N/N$ follows from (6.6) using the holomorphic resolvent $G(z)$ for large z . The small z region follows by analytical continuation. However, since $G(z)$ is multi-valued (already the simple case of the Ginibre-Girko ensemble yields two branches for the resolvent in (4.7)), the analytical continuation is ambiguous. The ambiguity may be removed by identifying $\log |Z_N|/N$ with some *generalized* “pressure” and taking $G(z)$ so that $\log |Z_N|/N$ is maximum⁴. As a result, $\log Z_N/N$ is piece-wise analytic in leading order in $1/N$ with “cusps” at

$$F^{(ij)}(x, y) \equiv V_N^{(i)}(x, y) - V_N^{(j)}(x, y) = 0, \quad (6.7)$$

following the transition from branch i to branch j of G with $V_N = \log |Z_N|/N$.

The character of the transition in the $1/N$ approximation can be highlighted by noting that for any finite N , the partition function (6.2) is a complex polynomial in z of degree N with random coefficients. In large N ,

$$V_N = \frac{1}{N} \log |Z_N| = \frac{1}{2} \int dv d\bar{v} \varrho(v, \bar{v}) \log |z - v|^2. \quad (6.8)$$

To leading order, the distribution of singularities along the “cusps” (6.7) is

³ A similar result can be obtained using a bozonized version to (6.2) in the Gaussian approximation.

⁴ This condition is equivalent to the saddle point condition. It does not necessarily fulfill the conditions discussed in [42].

$$\varrho(z, \bar{z}) = \frac{1}{2\pi} |\partial_z F|^2 \delta(F(z, \bar{z})) \quad (6.9)$$

which is normalized to 1 in the z -plane. Redefining the density of singularities by unit length along the curve $F(z, \bar{z}) = 0$, we may rewrite (6.9) as

$$\varrho(z, \bar{z})|_{F=0} = \frac{1}{2\pi} |\partial_z F| \equiv \frac{1}{4\pi} |G^{(i)} - G^{(j)}|. \quad (6.10)$$

For $\varrho \neq 0$, the integrand in (6.8) is singular at $z = v$ which results into different forms for V_N , hence a cusp. For $\varrho = 0$, that is $\partial_z F = 0$, V_N is differentiable. For physical V_N (real and monotonically increasing), the points $\varrho = 0$ are multicritical points. At these points all n -point ($n \geq 2$) functions diverge. This observation also holds for Ising models with complex external parameters [44]. Assuming macroscopic universality [10] for all n -points ($n \geq 2$), we conclude that $\partial_z F = 0$ means a branching point for the resolvents, hence $\partial_z G = \infty$ or $B'(G) = 0$ [31]. For hermitean matrices, these conditions coincide with the end-points of the eigenvalue distributions [31,32].

- *Example*

To illustrate the above concepts, consider the Ginibre-Girko ensemble of section 4.1. The resolvent in the holomorphic region satisfies (4.7), so

$$z = \tau G + \frac{1}{G}. \quad (6.11)$$

The integration (6.4) in E_0 is straightforward, and after fixing the asymptotic behavior we obtain

$$Z_N = G^{-N} e^{\frac{\tau}{2} N G^2} \left((1 - G^2(z)\tau)^{-\frac{1}{2}} + \mathcal{O}\left(\frac{1}{N}\right) \right). \quad (6.12)$$

Here G is the solution of (6.11). The pre-exponent in (6.12) follows from (6.6) with the matrix \mathcal{G} replaced by G and $\Gamma = \tau$, as seen in the “quark-quark” component of the vertex matrix in (4.1). Using (6.11) we observe that the pre-exponent diverges at two points in the z -plane, $z^2 = 4\tau$. At these points there is a “phase” change as we now show.

Given (6.12), the generalized “pressure” in leading order is

$$V_{\pm} = -\frac{1}{2} \log(G_{\pm} \bar{G}_{\pm}) + \frac{\tau}{4} (G_{\pm}^2 + \bar{G}_{\pm}^2) + \mathcal{O}\left(\frac{1}{N}\right). \quad (6.13)$$

V_{\pm} define two intersecting surfaces valued in the z -plane, for two branches G_{\pm} of the solutions to (6.11). The parametric equation for the intersecting curve is

$$F(z, \bar{z}) = V_+ - V_- = 0 \quad (6.14)$$

As indicated above, V_N is piece-wise differentiable. Note that $F = 0$ on the cut along the real axis, $-2\sqrt{\tau} < z < +2\sqrt{\tau}$, and from (6.10) the density of singularities per unit length is

$$\varrho(z, \bar{z})|_{F=0} = \frac{1}{\pi} \frac{\sqrt{4\tau - z^2}}{2\tau}. \quad (6.15)$$

Along F , the density of singularities is semi-circle. The density (6.15) vanishes at the end-points $z = \pm 2\sqrt{\tau}$. This is easily seen to be the same as $\partial_z G = \infty$, or $dB(G)/dG = 0$ with $B(G) = \tau G + 1/G$. As noted above the term in bracket in Eq. (6.12) vanishes at these points, with a diverging ‘‘quark-quark’’ contribution. The transition is fluctuation-driven. These points may signal the onset of scaling regions with possible universal microscopic behavior for nonhermitean random matrix models. This issue will be pursued elsewhere. At these points the $1/N$ expansion we have used breaks down.

Note that the case of the circular ensemble with $\tau = 0$ is very specific. From our analysis, we see that the support of F shrinks to a single point $z = 0$. In fact $Z_N = z^N$ to all orders in $1/N$. This can be understood by noting that since in

$$Z_N = \langle \det(z - \mathcal{M}) \rangle \quad (6.16)$$

the determinant is just

$$\det(z - \mathcal{M}) = \varepsilon_{i_1 i_2 \dots i_N} (z - \mathcal{M})_{i_1}^1 (z - \mathcal{M})_{i_2}^2 \dots (z - \mathcal{M})_{i_N}^N \quad (6.17)$$

all expectation values vanish (exactly to all orders in $1/N$) for random gaussian complex matrices, *i.e.*

$$\langle \mathcal{M}_b^a \mathcal{M}_d^c \dots \mathcal{M}_y^x \rangle = 0. \quad (6.18)$$

Hence our claim.

The present construction for the partition function for the Ginibre-Girko ensemble extends to the other cases of nonhermitean ensembles with unitary randomness. We briefly mention the case of chiral random ensembles plus

deterministic nonhermitean matrix of (off-diagonal) strength ζ . The relevant one- and two-point correlators in the holomorphic and nonholomorphic domains were explicitly constructed in sections 4.3, 5.4 and 5.5. Using these results and in analogy with (6.6), elementary integration for this case leads to

$$Z_N(z, \zeta) = e^{NE_0} \cdot \left(\left\{ D^{-2}[(D + \zeta^2)^2 - (z - G)^4] \right\}^{-\frac{1}{2}} + \mathcal{O}\left(\frac{1}{N}\right) \right), \quad (6.19)$$

where $D = (z - G)^2/G^2$, and

$$E_0(z, \zeta) = G^2 + \log \frac{z - G}{G} \quad (6.20)$$

with the appropriate branch of holomorphic G solution to (4.28), with $\mu = \zeta$. Note that for $z = 0$ and $G^2 = -1 - \zeta^2$, the pre-exponent in (6.19) diverges. It also diverges at $z = z_*$ which are the zeros of (6.10) for the present case (two zeros for small ζ and four zeros for large ζ). Again, at these points, the $1/N$ expansion breaks down marking the onset of scaling regions and the possibility of microscopic universality. The $z = 0$ divergence is just the notorious ‘‘Goldstone’’ mode in chiral models, illustrating the noncommutativity of $N \rightarrow \infty$ and $z \rightarrow 0$. The rest of the arguments follow easily from the preceding example, in agreement with the ‘‘thermodynamics’’ discussed in [43].

- *Replicas*

We note that in the circular case, the partition function with N_f ‘‘replicas’’

$$Z_{N, N_f} = \left\langle \det^{N_f}(z - \mathcal{M}) \right\rangle \quad (6.21)$$

yields simply

$$Z_{N, N_f} = z^{N N_f} \quad (6.22)$$

For general \mathcal{M} and N_f noninteger the determinant in (6.21) is multivalued, and a determination is in general needed. Here, it will be assumed by *interpolating* the integer result [43]⁵. While the limits $N \rightarrow \infty$ and $N_f \rightarrow 0$ are compatible for $\ln Z_{N, N_f}/N$ through the diagrammatic analysis, it is not necessarily the case for the connected functions (z -derivatives) since singularities for $z \sim \mathcal{M}$ are generated.

⁵ Another way is to use the ξ -function in combination with the heat-kernel construction, through $\det^{N_f} A = e^{-N_f \xi'_A(0)}$ and $\xi_A(s) = \text{Tr}(1/A^s)$. We have checked that the leading term is in agreement with the interpolation for smooth operators.

In the $1/N$ expansion, the “quark” insertions are suppressed by powers of N_f/N for singularity-free operators. In general, this implies that random matrix models are self-quenched [43], and holomorphy in the external parameter z is preserved as $N \rightarrow \infty$ (modulo cusps). In the presence of singularities, holomorphic symmetry is usually upset as $N \rightarrow \infty$ for a certain range of N_f and $z \sim \mathcal{M}$, and arguments similar to those of section 3 should be used. This confirms the shortcomings of (6.21) to yield the quenched one-point functions [23], and two-point functions [34] for small z .

6.2 Nonholomorphic Z

The above analysis for the holomorphic thermodynamical potential may also be extended to nonholomorphic partition functions, again for Gaussian unitary randomness. For example,

$$Z_N[z, \bar{z}] = \langle \det |z - \mathcal{M}|^2 \rangle = \left\langle \int d\psi d\bar{\psi} d\phi d\bar{\phi} e^{-\bar{\psi}(z - \mathcal{M})\psi - \bar{\phi}(\bar{z} - \mathcal{M}^\dagger)\phi} \right\rangle \quad (6.23)$$

which is the random matrix analogue of the partition function discussed in [45] for unquenched QCD. In these partition functions the phase of the ($N_f = 2$) determinant is set to one. Again, the one- and two-point functions may be obtained from $\log Z_N$ by differentiation with respect to z and \bar{z} (modulo delta functions).

From (6.1) we have

$$G(z, \bar{z}) = \frac{\partial E_0(z, \bar{z})}{\partial z} \quad \bar{G}(z, \bar{z}) = \frac{\partial E_0(z, \bar{z})}{\partial \bar{z}} \quad (6.24)$$

These expressions may be integrated and the integration constant is set by the matching condition

$$E_0 \sim \log |z|^2 \quad \text{for } z \rightarrow \infty. \quad (6.25)$$

For the Ginibre-Girko ensemble the nonholomorphic resolvent (4.2) yields

$$E_0(z, \bar{z}) = \frac{1}{1 - \tau^2} \left[|z|^2 - \frac{1}{2}\tau(z^2 + \bar{z}^2) \right] + c_{nh} \quad (6.26)$$

while the holomorphic resolvent (4.7) gives

$$E_0(z, \bar{z}) = \frac{z}{4\tau} \left(z \mp \sqrt{z^2 - 4\tau} \right) \pm \log \left[\frac{1}{2}(z + \sqrt{z^2 - 4\tau}) \right] + h.c. + c_h \quad (6.27)$$

with the limit

$$\lim_{z \rightarrow \infty} E_0(z, \bar{z}) = 1 + \log |z|^2 + c_h. \quad (6.28)$$

The constant c_h is -1 , and c_{nh} is determined from the continuity condition of E_0 at the boundary (4.9). At $\tau = 0$

$$E_0 = \begin{cases} \log |z|^2 & : |z|^2 > 1 \\ |z|^2 - 1 & : |z|^2 < 1 \end{cases}. \quad (6.29)$$

The “phase” change at $|z| = 1$ is fluctuation-driven.

The expression for the correlator in the holomorphic phase follows by differentiating the term E_1 , that is

$$\partial_z \partial_{\bar{z}} E_1 = \langle \text{tr} \left| \frac{1}{z - \mathcal{M}} \right|^2 \rangle_c \quad (6.30)$$

Hence

$$E_1 = -\ln \det(1 - \mathcal{G} \otimes \bar{\mathcal{G}}^T \cdot \Gamma) + \Phi \quad (6.31)$$

where Φ is a harmonic function. To determine Φ we note that

$$\partial_z E_1 = G_1(z), \quad (6.32)$$

$G_1(z)$ is the $1/N$ correction to the one-point function in the planar approximation. It follows from the insertion of “quark” or “conjugate-quark” loops in $G(z)$. Specifically

$$G_1 = -\text{tr} \left[\frac{1}{1 - \mathcal{G} \otimes \bar{\mathcal{G}}^T \cdot \Gamma} \partial_z (\mathcal{G} \otimes \bar{\mathcal{G}}^T \cdot \Gamma) + \frac{1}{2} \frac{1}{1 - \mathcal{G} \otimes \mathcal{G}^T \cdot \Gamma} \partial_z (\mathcal{G} \otimes \mathcal{G}^T \cdot \Gamma) \right], \quad (6.33)$$

which can be rewritten as

$$\partial_z \left\{ \ln \det(1 - \mathcal{G} \otimes \bar{\mathcal{G}}^T \cdot \Gamma) + \frac{1}{2} \ln \det(1 - \mathcal{G} \otimes \mathcal{G}^T \cdot \Gamma) \right\}. \quad (6.34)$$

A similar expression follows from \bar{G} . Hence

$$E_1 = -\frac{1}{2} \log \det(1 - \mathcal{G} \otimes \bar{\mathcal{G}}^T \cdot \Gamma) - \frac{1}{2} \log \det(1 - \mathcal{G} \otimes \mathcal{G}^T \cdot \Gamma)$$

$$-\frac{1}{2} \log \det(1 - \mathcal{G} \otimes \mathcal{G}^T \cdot \Gamma) - \frac{1}{2} \log \det(1 - \overline{\mathcal{G}} \otimes \overline{\mathcal{G}}^T \cdot \Gamma). \quad (6.35)$$

As a result, the partition function (6.23) reads

$$Z_N[z, \bar{z}] = e^{NE_0} \cdot \left(\left\{ \det(1 - \mathcal{G} \otimes \overline{\mathcal{G}}^T \cdot \Gamma) \mid \det(1 - \mathcal{G} \otimes \mathcal{G}^T \cdot \Gamma) \right\}^{-1} + \mathcal{O}\left(\frac{1}{N}\right) \right). \quad (6.36)$$

Note that the contributions from the wheel-diagrams are of the form $1/\sqrt{\det}$ and hence “bosonic” in character. In (6.35), there are two contributions from the “quark-conjugate-quark” wheels (upper line in (6.35)), one contribution from the “quark-quark” wheel and one contribution from the “conjugate-quark-conjugate-quark” wheel, thereby explaining all contributions in (6.36) at next to leading order. Like in the holomorphic case, again similar results can be obtained using a bozonized version to (6.23) in the Gaussian approximation.

Again, the partition function Z_N has an essential singularity in $1/N$, but $\log Z_N/N$ does not. For any finite N , the latter diverges for

$$\det(1 - \mathcal{G} \otimes \overline{\mathcal{G}}^T \cdot \Gamma) = 0 \quad (6.37)$$

The divergence condition from the second pre-exponent in (6.36), *i.e.*

$$\det(1 - \mathcal{G} \otimes \mathcal{G}^T \cdot \Gamma) = 0 \quad (6.38)$$

is not essential, since the line of singularities following from (6.37) defines the boundary of a surface that in general contains the cusps at $\partial_z G = \infty$. In particular, the set of discrete points (6.38). In this case, the transition in the z -plane is fluctuation-driven. For the Ginibre-Girko example, the nonholomorphic partition function diverges according to (6.37), that is for

$$1 - |G|^2 = 0 \quad (6.39)$$

Indeed in the holomorphic region, we could replace \mathcal{G} by G , the modulus follows from the “conjugate-quark” resolvent, and the vertex corresponds to the “quark-conjugate-quark” element of the kernel (4.1) set to 1. The line of singularities (6.39) reproduces in this case the ellipse (4.9). The ellipse includes the points of the “phase” change, *i.e.* the focal points $z^2 = 4\tau$, connected by the interval (6.14), *i.e.* $F = 0$. We recall that these focal points were obtained as a divergence condition for (6.12), a special case of the general condition (6.38).

The same results were also discussed in [34] for the case of a chiral random matrix model with a chemical potential $\mu = \zeta$ in the quenched approximation.

In particular, it was shown that the condition (6.37) exactly reproduces the islands of “mixed-condensate”, obtained using the replica methods [23]. In this case the condition (6.37) reads [34]

$$D^{-2}[(D - \zeta^2)^2 - |z - G|^4] = 0 \quad (6.40)$$

with $D = |(z - G)/G|^2$, therefore exactly the condition (5.41). Comparing to the “quark-quark” correlator in (6.19), we notice the appearance of the modulus and the flip in the sign of ζ due to the fact that now we measure the correlation between the “quark” and the “conjugate-quark”. Equation (6.40) defines the boundaries of the fore mentioned “islands”. Inside (6.40), the resolvents in (6.36) are nonholomorphic, while outside (6.40) they are holomorphic. The holomorphic and nonholomorphic resolvents match on (6.40).

7 Conclusions

We have shown that chiral and hermitean random matrix models are amenable to diagrammatic techniques in the context of the $1/N$ approximation. Since the matrices are hermitean, the eigenvalue distributions and their macroscopic correlations follow from one- and two-point functions that are analytic in the complex z -plane modulo isolated singularities. Although our results were carried using “quenched” measures, we expect them to hold for “unquenched” ones as well since the “quark” effects are $1/N$ suppressed [43].

We have shown how to extend the diagrammatic arguments of Brézin, Hikami and Zee to a large variety of nonhermitean random matrix models. For nonhermitean matrices, the one- and two-point correlation functions are analytic in the complex z -plane modulo surface singularities. These singularities originate from an accumulation of eigenvalues in the large N limit, and cause the one- and two-point functions to be nonholomorphic in finite domains. The breakdown condition is set by the divergence of the correlations between pairs of eigenvalues, conjugate of each other and a distance N apart in the spectrum [34]. We have explicitly constructed the one- and two-point functions in the planar approximation and shown that the analytical results are reproduced by direct numerical calculations using large samples of random and nonhermitean matrices.

We have explicitly shown how the partition functions of nonhermitean matrix models with unitary randomness can be related to the one- and two-point functions for holomorphic as well as nonholomorphic kernels to order $\mathcal{O}(1/N)$, thereby providing a simple physical interpretation to several preceding results. The partition functions to the order calculated are solely a function of the resolvent G . We expect this property to hold to higher orders, and even suspect

a generalized form of macroscopic universality when extended to non-Gaussian weights [10]. Generic equations for the singularities of the partition functions were found both for the holomorphic as well as the nonholomorphic cases to order $\mathcal{O}(1/N)$. These singularities are related to structural changes in the random matrix model, such as changes in the eigenvalue distributions and correlations in models with [23,34] or without dissipation [32,43]. Our construction may be useful for investigating a number of related issues in random matrix and polynomial models [46].

Acknowledgements

This work was partially supported by the US DOE grant DE-FG-88ER40388, by the Polish Government Project (KBN) grant 2P03004412 and by the Hungarian Research Foundation OTKA grants T022931 and F019689. The authors would like to thank Jurek Jurkiewicz for discussions. I.Z. thanks Robert Schrock for a discussion. G.P. thanks the Soros Foundation for financial support and the Nuclear Theory Group at Stony Brook for hospitality. R.A.J. would like to thank the Nuclear Theory Group at Stony Brook and GSI, where part of this work was done.

Note Added

After submission of this work, some of our results were confirmed by other authors. Our diagrammatic approach and part of our results have been confirmed in two interesting papers by Feinberg and Zee, cond-mat/9701387 and cond-mat/9704191. The analytical results of section 6 as illustrated in our second example and the discussion on the replicas, account for the nature and location of all singularities and their distribution as they appeared in an extensive numerical analysis (up to 500 digits accuracy) by Halasz et al., hep-lat/9611008 and hep-lat/9703006.

References

- [1] K. Slevin and T. Nagao, Phys. Rev. Lett. **70** (1993) 635, and references therein.
- [2] see e.g. M.L. Mehta, *Random matrices* (Academic Press, New York, 1991); C.E. Porter, *Statistical Theories of Spectra: Fluctuations* (Academic Press, New York, 1969).

- [3] C. Itoi, *Universal wide correlators in non-gaussian orthogonal, unitary and symplectic random matrix ensembles*, eprint cond-mat/9611214; Ch. Itoi, H. Mukaida and Y. Sakamoto, *Replica method for wide correlations in gaussian orthogonal, unitary and symplectic random matrix ensembles*, e-print cond-mat/9612228.
- [4] M. Nowak, J.J.M. Verbaarschot and I. Zahed, Phys. Lett. **B217** (1989) 157; Yu A. Simonov, Phys. Rev. **D43** (1991) 3534; E.V. Shuryak and J.J.M. Verbaarschot, Nucl. Phys. **A560** (1993) 306; J.J.M. Verbaarschot and I. Zahed, Phys. Rev. Lett. **70** (1993) 3852.
- [5] see Y.V. Fyodorov, B.A. Khoruzhenko and H.-J. Sommers, Phys. Lett. **A226** (1997) 46, and references therein.
- [6] Y. V. Fyodorov and H.-J. Sommers, *Statistics of resonance poles, phaseshifts and time delays in quantum chaotic scattering*, (to be published in J. Math. Phys.)
- [7] see P. Di Francesco, P. Ginsparg and J. Zinn-Justin, Phys. Rept. **254** (1995) 1, and references therein.
- [8] K.B. Efetov, Adv. in Phys. **32** (1983) 53; J.J.M. Verbaarschot, H.A. Weidenmüller and M. R. Zirnbauer, Phys. Rep. **129** (1985) 367.
- [9] J.J.M. Verbaarschot, H. A. Weidenmüller and M. Zirnbauer, Ann. Phys. (NY) **153** (1984) 153; For recent applications see e.g. P.G. Silvestrov, *Summing the graphs for random band matrices*, e-print cond-mat/9610064; C.W. Brouwer and C.W.J. Beenakker, J. Math. Phys. **37** (1996) 4904; see also Ref.[11].
- [10] J. Ambjørn, J. Jurkiewicz and Yu.M. Makeenko, Phys. Lett. **B251** (1990) 517.
- [11] E. Brézin and A. Zee, Phys. Rev. **E49** (1994) 2588; E. Brézin and A. Zee, Nucl. Phys. **B453** (1995) 531; E. Brézin, S. Hikami and A. Zee, *Universal correlations for deterministic plus random Hamiltonians*, e-print hep-th/9412230.
- [12] J. Ginibre, J. Math. Phys. **6** (1965) 440; see also V.L. Girko, *Spectral theory of random matrices (in Russian)*, (Nauka, Moscow, 1988).
- [13] D. Voiculescu, Invent. Math. **104** (1991) 201; D.V. Voiculescu, K.J. Dykema and A. Nica, *Free Random Variables*, (Am. Math. Soc., Providence, RI, 1992).
- [14] G. 't Hooft, Nucl. Phys. **B75** (1974) 464.
- [15] L.A. Pastur, Theor. Mat. Phys. (USSR) **10** (1972) 67.
- [16] F. Wegner, Phys. Rev. **B19** (1979) 783.
- [17] see e.g. D. Diakonov, *Chiral symmetry breaking by instantons*, e-print hep-ph/9602375; T. Schäfer and E.V. Shuryak, *Instantons in QCD*, e-print hep-ph/9610451; M.A. Nowak, M. Rho and I. Zahed, *Chiral Nuclear Dynamics* (World Scientific, Singapore, 1996).
- [18] A. Casher and H. Neuberger, Phys. Lett. **B139** (1984) 67.

- [19] J. Jurkiewicz, M.A. Nowak and I. Zahed, Nucl. Phys. **B478** (1996) 605.
- [20] H.-J. Sommers, A. Crisanti, H. Sompolinsky and Y. Stein, Phys. Rev. Lett. **60** (1988) 1895.
- [21] B.A. Khoruzhenko, J. Phys. A. Math. Gen. **29** (1996) L165.
- [22] I. Barbour et al., Nucl. Phys. **B275** (1996) 296; C.T.H. Davies and E.G. Klepfish, Phys. Lett. **B256** (1991) 68; J.B. Kogut, M.P. Lombardo and D.K. Sinclair, Phys. Rev. **D51** (1995) 1282.
- [23] M. Stephanov, Phys. Rev. Lett. **76** (1996) 4472; M. Stephanov, *Dirac operator as a random matrix and the quenched limit of QCD with chemical potential*, e-print hep-lat 9607060.
- [24] C. Mahaux and H.A. Weidenmüller, *Shell-model approach to nuclear reactions*, (North Holland, Amsterdam, 1969).
- [25] F. Haake, F. Izrailev, N. Lehmann, D. Saher and H.-J. Sommers, Zeit. Phys. **B88** (1992) 359.
- [26] N. Lehmann, D. Saher, V.V. Sokolov and H.-J. Sommers, Nucl. Phys. **A582** (1995) 223.
- [27] P. Neu and R. Speicher, J. Phys. **A28** (1995)L79; A. Nica and R. Speicher, Amer. J. Math. **118** (1996) 799.
- [28] M. Douglas, *Large N gauge theory: expansions and transitions*, e-print hep-th/9409098.
- [29] R. Gopakumar and D.J. Gross, Nucl. Phys. **B451** (1995) 379.
- [30] M. Engelhardt, Nucl. Phys, **B481** (1996) 479.
- [31] A. Zee, Nucl. Phys. **B474** (1996) 726.
- [32] M.A. Nowak, G. Papp and I. Zahed, Phys. Lett. **B389** (1996) 137; R.A. Janik, M.A. Nowak, G. Papp and I. Zahed, *The $U(1)$ problem in chiral random matrix models*, e-print hep-lat/9611012; to be published in Nucl. Phys. **B**.
- [33] R.A. Janik, M.A. Nowak, G. Papp, J. Wambach and I. Zahed, Phys. Rev. **E55** (1997) 4100.
- [34] R.A. Janik, M.A. Nowak, G. Papp and I. Zahed, Phys. Rev. Lett. **77** (1996) 4876.
- [35] E. Brézin and A. Zee, Nucl. Phys. **402** (1993) 613.
- [36] G. Akemann and J. Ambjørn, J. Phys. **A29** (1996) L555; G. Akemann, Nucl. Phys. **B482** (1996) 403; G. Akemann, *Universal correlations for multi-arc complex matrix models*, e-print hep-th/9702005.
- [37] E. Brézin and S. Hikami, *Spectral form factor in a random matrix theory*, e-print cond-mat/9608116.

- [38] J.B. French, P.A. Mello and A. Pandey, *Ann. Phys. (N.Y.)* **113** (1978) 277; J.J.M. Verbaarschot, H.A. Weidenmüller and M. Zirnbauer, *Ann. Phys. (N.Y.)* **153** (1984) 367.
- [39] J. Ambjørn, C.F. Kristjansen and Yu.M. Makeenko, *Mod. Phys. Lett.* **A7** (1992) 3187.
- [40] L. McLerran and A. Sen, *Phys. Rev.* **D32** (1985) 2794; T.H. Hansson and I. Zahed, *Phys. Lett.* **B309** (1993) 385; J.V. Steele, A. Subramanian and I. Zahed, *Nucl. Phys.* **B452** (1995) 545; J.V. Steele and I. Zahed, unpublished.
- [41] J. Ambjørn, L. Chekhov, C.F. Kristjansen and Yu. Makeenko, *Nucl. Phys.* **B404** (1993) 127.
- [42] K. Huang, *Statistical Mechanics*, (John Wiley, New York, 1987).
- [43] R.A. Janik, M. A. Nowak and I. Zahed, *Phys. Lett.* **B392** (1997) 155; R.A. Janik, M. A. Nowak, G. Papp and I. Zahed, *Acta Phys. Pol.* **B27** (1996) 3271; M. A. Nowak, M. Rho and I. Zahed, *Chiral Nuclear Dynamics*, (World Scientific, Singapore, 1996).
- [44] R. Schrock, private communication; G. Marchesini and R. Schrock, *Nucl. Phys.* **B318** (1989) 541; V. Matveev and R. Schrock, *J. Phys.* **A28** (1995) 1557; *Nucl. Phys. (Proc. Suppl.)* **B42** (1995) 776.
- [45] A. Gocksch, *Phys. Rev. Lett.* **61** (1988) 2054.
- [46] J. Jurkiewicz, *Phys. Lett.* **B245** (1990) 178; M. Staudacher, *Nucl. Phys.* **B336** (1990) 349; B. Derrida, *Physica* **A177** (1991) 31; E. Bogomolny, O. Bohigas and P. Lebcief, *Jour. Stat. Phys.* **85**(1996) 639.